DIPLOMARBEIT

Characterization of the redox environment in protein refolding processes

ausgeführt zum Zwecke der Erlangung des akademischen Grades eines Master of Science (MSc) unter der Leitung von

Associate Prof. Dipl.-Ing. Dr. Oliver SPADIUT

betreut durch

Projektass. Igwe CHIKA MSc

Institut für Verfahrenstechnik, Umwelttechnik und Technische Biowissenschaften

Technischen Universität Wien
Fakultät für Technische Chemie

von

Dominik DEUSCHITZ, BSc, BSc
[redacted]

Wien, am	Unterschrift des Betreuers	eigenhändige Unterschrift

Eidesstattliche Erklärung

Hiermit erkläre ich, dass ich diese Diplomarbeit selbstständig verfasst habe, dass ich die verwendeten Quellen vollständig angegeben habe und dass ich Zitate die anderen Publikationen im Wortlaut oder dem Sinn nach entnommen sind, unter Angabe der Herkunft als Entlehnung kenntlich gemacht habe.

Wien, am

eigenhändige Unterschrift

Abstract

Protein refolding, is often done via an empirical approach rather than a Quality by Design approach. Quality by Design aims to improve process understanding and robustness by identifying critical process parameters and, ideally, linking them to desired critical quality attributes. The redox potential represents an interesting parameter for a possible process analytical technology tool, since the formation of disulfide bonds occurs via a redox reaction and since *in vivo* folding processes are reported to be influenced by the redox potential. Oxygen is a cost-effective oxidant and, furthermore, it can support the formation of disulfide bonds, so its effect was also investigated. In order to avoid the influence of air/water interfaces, bubble free control strategies for the dissolved oxygen were developed. In this work, the control of the redox potential was carried out exclusively via the dissolved oxygen, since no alternative oxidant could be found for the galactose oxidase. Consequently, the parameters were not considered independently of each other. With the developed control strategies, several reactor runs were performed under controlled conditions. A decrease in activity was observed with increasing dissolved oxygen as well as increasing redox potential. Only under oxygen-free conditions and a low redox potential, an increase in activity could be measured over several hours. Both parameters could not be mathematically linked to the activity, but further critical process parameters were found, which probably allow a linkage. The dissolved oxygen or the redox potential show an influence on the enzymatic activity and should, in refolding processes, therefore be observed or controlled. Since both parameters could not be considered independently and they correlate with each other, the influence cannot be attributed exactly. Another parameter that turned out to be promising is the free thiol concentration, which is composed of the cysteines of the protein and the cysteamine of the refolding buffer. In the future, this parameter could possibly be determined by a model that takes into account the redox potential, the dissolved oxygen and the amount of reductant used, which could lead to a better understanding of the process.

German version

Protein refolding, erfolgt oft über einen empirischen Ansatz und nicht über einen Quality by Design Ansatz. Quality by Design zielt darauf ab, das Prozessverständnis und die Robustheit zu verbessern, indem kritische Prozessparameter identifiziert und idealerweise mit gewünschten kritischen Qualitätsattributen verknüpft werden. Das Redoxpotential stellt einen interessanten Parameter für ein mögliches Process Analytical Technology tool dar, da die Ausbildung von Disulfid Bindungen über eine Redoxreaktion erfolgt und da bei *in vivo* folding Prozessen von einem Einfluss des Redoxpotentials berichtet wird. Ein kosteneffizientes Oxidationsmittel ist Sauerstoff und des Weiteren, kann dieser die Ausbildung von Disulfid Bindungen unterstützen, daher wurde auch dessen Effekt untersucht. Um den Einfluss von Luft/Wasser Grenzflächen vermeiden zu können, wurden blasenfreie Kontrollstrategien für den Gelöstsauerstoff entwickelt. Die Kontrolle des Redoxpotentials erfolgte in der Arbeit ausschließlich über den Gelöstsauerstoff, da kein alternatives Oxidationsmittel für die Galaktoseoxidase gefunden werden konnte, folglich wurden die Parameter nicht unabhängig voneinander betrachtet. Mit den entwickelten Kontrollstrategien wurden mehrere Reaktorversuche bei kontrollierten Bedingungen durchgeführt. Dabei konnte mit steigenden Gelöstsauerstoff als auch steigenden Redoxpotential eine Abnahme der Aktivität beobachtet werden. Nur bei sauerstofffreien Bedingungen und einem möglichst niedrigen Redoxpotential, konnte eine Zunahme der Aktivität über mehrere Stunden gemessen werden. Beide Parameter konnten zwar nicht mathematisch mit der Aktivität verknüpft werden, allerdings konnten weitere kritische Prozessparameter gefunden werden, die voraussichtlich eine Verknüpfung ermöglichen. Der Gelöstsauerstoff bzw. das Redoxpotential zeigen einen Einfluss auf die enzymatische Aktivität und sollten, bei refolding Prozessen, daher beobachtet oder kontrolliert werden. Da beide Parameter nicht unabhängig voneinander betrachtet werden konnten und diese miteinander korrelieren, kann der Einfluss nicht exakt zugeschrieben werden. Ein weiterer Parameter der sich als vielversprechend herausstellte ist die freie Thiol Konzentration, welche sich aus dem Cysteinen des Proteins und dem Cysteamin des Refolding Buffers zusammensetzt. Dieser Parameter könnte zukünftig eventuell über ein Model ermittelt werden, welches das Redoxpotential, den Gelöstsauerstoff und die eingesetzte Reduktionsmittelmenge berücksichtigt, wodurch ein besseres Prozessverständnis erlangt werden könnte.

Acknowledgments

First of all, I would like to thank Assoc. Prof. Oliver Spadiut for the great opportunity to do this work. Furthermore, I would like to thank my supervisor, Igwe Chika, for her strong support in planning and performing the experiments. Special thanks also go to Müller Don Fabian and Pauk Jan Niklas, who assisted me in the use of Python and modeling. Without the practical help of Mira Jaeger and Teubel Marcel, the measurement intervals during the reactor experiments would not have been possible. Therefore, I would also like to thank them.

I also want to acknowledge financial support through the COMET Centre CHASE, funded within the COMET - Competence Centers for Excellent Technologies programme by the BMK, the BMDW and the Federal Provinces of Upper Austria and Vienna, is gratefully acknowledged. The COMET programme is managed by the Austrian Research Promotion Agency (FFG).

List of Abbreviations

3MBA	3-methoxybenzyl alcohol
ABTS	2,2'-azino-bis(3-ethylbenzothiazoline-6-sulfonic acid
CPP	critical process parameters
CQA	critical quality attributes
Cys	cysteine
DO	dissolved oxygen
DoE	Design of Experiment
DTNB	5,5-dithio-bis-(2-nitrobenzoic acid)
E.coli	Escherichia coli
FDA	US Food and Drug Administration
GalOx	galaktose oxidase
GSH	glutathione
GSSG	glutathione disulfide
His	histidine
HPLC	high-performance liquid chromatography
HRP	Horseradish Peroxidas
IB	Inclusion bodies
ICH	International Council for Harmonisation of Technical Requirements for Pharmaceuticals for Human Use
LMW disulfid	low molecular weight disulfid
LMW thiol	low molucular weight thiol
MS	mass spectrometry
OLS	Ordinary least squares
OPC	Open Platform Communications
ORP	oxidation-reduction potential
QbD	Quality by Design
PAT	Process Analytical Technology
PLA	polylactic acid
PLS	Partial least squares
TCEP	tris(2-carboxyethyl)phosphine
TFA	trifluoroacetic acid
TNB	2-nitro-5-thiobenzoates
TRP	tryptophan
Tyr	tyrosine

Contents

1 Introduction

The introduction of human insulin opened a new door for drugs. Today, protein and peptide drugs account for 10 % of the pharmaceutical market. The US Food and Drug Administration (FDA) has already approved 239 therapeutic proteins and peptides for clinical use.[81] The recombinant protein market recorded a total estimated value of 1.75 billion in 2021. Furthermore, an average growth rate of 12 % is assumed until 2030.[62] Proteins as therapeutics have generated a high level of attention as they are involved in a variety of biochemical reactions and show high specificity.[81] In simple terms, to produce a recombinant protein, a DNA sequence is introduced into an expression vector, which in turn is introduced into a host. The host can then express a protein according to the introduced DNA, which enables the targeted production of proteins.[64] A very popular host for the production of recombinant proteins is *Escherichia coli* due to its rapid growth kinetics, inexpensive cultivation, and ease of manipulation. Drawbacks of *E. coli* include codon bias, inclusion body formation, toxicity, protein inactivity, mRNA instability, and lack of post-translational modifications.[43] For the expression of a recombinant protein, elevated temperatures, high inducer concentrations, and strong promoter systems are often used to achieve a high translation rate. This places a high stress on the bacterial quality control system, leading to the formation of partially folded and misfolded proteins. Furthermore, the reducing environment of the cytosol, the lack of eukaryotic chaperonins and a lack of post-translational modifications pose a problem for the formation of functional recombinant proteins, which can lead to the formation of so-called inclusion budies (IBs). They occur due to the accumulation of misfolded and partially folded recombinant protein.[71]

1.1 Challenges and potential of inclusion bodies

In the industrial production of a recombinant protein, the fermentation parameters temperature, dissolved oxygen (DO), pH, media compositions and feeding strategy are usually optimized to maximize the product yield. [50, 78] However, not only the quantity of the produced protein is crucial, but also the quality plays a significant role. In particular, the correct folding of the recombinant protein as well as its *in vivo* stability are critical factors to be considered when optimizing the process parameters. Setting the fermentation parameters for maximum production yield can negatively affect the quality of the recombinant protein.[2] Due to the high expression levels aimed at during fermentation, the quality of the recombinant protein is reduced, which can be seen in the form of partially folded or incorrectly folded proteins. These incorrectly folded proteins then aggregate to IBs, which often show no activity.[71] Consequently,

IBs tend to be avoided in the production of soluble native protein. Reducing IBs production can be done in a variety of ways. Lowering the temperature during production can reduce IB production, as the lower temperature leads to a slowing of the expression rate.[14, 70, 89] However, increasing the temperature can also lead to a lower IB production rate, as a heat shock can increase the production of chaperones, which can support the folding of the recombinant protein.[41] Therefore, a specific strategy must be found individually for a host with its specific recombinant protein to avoid IBs. There are a variety of different approaches to reduce the formation of IBs, such as reduction of the inducer, addition of glucose to the medium, addition of chemical additives, control of pH, optimization of the expression vector, etc.[8] Many of these approaches function by reducing the rate of expression. Despite optimization of fermentation conditions for soluble native protein, IBs still form as a by-product in *E. coli*.[73] IB formation has been reported to occur in around 40 % of recombinant protein production processes.[45] For a long time, these were considered an undesirable by-product. [73] However, this view has changed in the last decades due to several aspects. The production of substances toxic to the host organism is difficult, since the product formed harms the hosts themselves. Therefore, production via IBs, is very interesting, since IBs often show no activity. For that reason , such a production method would be suitable for antibacterial, antiviral, antifungal and antiparasitic compounds to keep production costs low, which will become important considering the increase of multiresistant microbes.[8] Another very interesting aspect is the possibility to generate higher yields via the production of IBs than via the production of the soluble native protein. As already mentioned, the expression rate of the recombinant protein is often reduced to minimize the formation of IBs, which also causes a decrease in the space time yield.[8, 2] Since maximum production conditions can be aimed for the fermentation of IBs, it is conceivable to generate higher yields via the production of IBs than in the production of soluble native protein. In an experiment with HRP it was shown that a 20 times higher yield could be achieved by the production of IBs compared to the soluble native product.[37] Furthermore, IBs are often easily separable from the rest of the cells, as they differ in density from the rest of the cell population.[31, 71] IBs also show resistance to proteases, which reduces the degradation of the recombinant protein.[72] Two critical factors of the product quality of a recombinant protein are its 3-dimensional folding and possible postranslational modifications. These properties have to be subsequently adapted in IBs. This refolding and introduction of prostranslational modifications is an essential task in which several challenges have to be overcome.[2]Protein refolding on an industrial scale has several inefficient aspects, which are often due to protein aggregations. To deal with this, the industry often uses large volumes and expensive additives, but still only low yields of 18-25 % are often obtained, which is problematic from an economic perspective.[91]

1.2 Special challenge disulfide bonds

Disulfide bonds are a post-translational modification in which two cysteines are covalently bonded together. These bonds have a typical length of about 2.0 A.[18] They are an important structural element, which influences the stability of the 3-D structure and can have a relevant redox activity.[11] Their absence or cleavage can lead to a breakdown of the native form of the protein as well as to a loss of function. Furthermore, the absence or non-native linkage can lead to protein aggregates. Approximately 18% of human proteins on uniprot have at least one disulfide bond, which is not an irrelevant part of the human proteome.[85] Looking at the biosimilars approved by the EU in the years 2021-2022, 15 biosimilars were approved in these years (6 different active substances, see appendix table5.1), all of which are expected to have disulfide bonds (comparison with uniprot). This indicates a high frequency of disulfide bonds, in recombinant protein in the pharmaceutical industry. Recombinant proteins with disulfide bonds present a particular challenge in refolding. In IBs disulfide bonds may not be bound according to the native form and therefore must be broken and then properly assembled during refolding, which presents an additional challenge in refolding.[71, 55] Proteins that have disulfide bonds in their native form are unstable in their reduced form without disulfide bonds and tend to form aggregates.[32] The refolding process results in the formation of native protein and the formation of by-products such as aggregates and misfolded protein. Aggregation can occur due to intermolecular interactions of intermediates, which are due to hydrophobic regions in the protein or covalent disulfide bonds. To minimize this type of aggregation, refolding should occur away from intermediates that are prone to aggregation.[55]

1.3 Characteristic of inclusion bodies

IBs are microscopic intracellular particles in the size range of 0.2 to 1.5 µm. They consist predominantly of recombinant protein, which may be either partially folded or misfolded.[45] In addition, components of the bacterial membrane, other host cell proteins, and RNA may be present in the IBs.[71] Under the electron microscope, the surface of these particles appears either rough or smooth and they do not show a regular structure. [16] Usually, IBs accumulate in the cytoplasm, but can also be found in the periplasmic space.[3] In *E. coli*, the IBs are concentrated at the poles of the cell, resulting in an asymmetric distribution between the daughter cells. As a result, the daughter cell with a lower amount of IBs has a higher growth rate.[61] As mentioned earlier, high stress conditions during the production of the recombinant protein play an important role in the formation of IBs. In addition, the amino acid sequence of the recombinant protein also influences the formation of these particles. In particular, highly hydrophobic proteins are more prone to the formation of IBs. [71, 61]

1.4 Inclusion body processing workflow

The conventional strategy to obtain native protein from IBs consists of four main steps: Isolation of the purified IBs, solubilization of the IBs, refolding of the solubilized proteins, and purification of the refolded proteins. [71] Since IBs are usually located inside the cell, the cells must first disrupted before these four main steps, which is done via an appropriate combination of mechanical and chemical influences. IBs have a higher density compared to the rest of the cell population, which allows them to be isolated via centrifugation. Through several washing steps impurities can be removed. For example, washing with Triton x100 and deoxy-cholic acid can wash out membrane components. The purity of the IBs is relevant for several aspects. On the one hand impurities can interfere with protein refolding and on the other hand a higher IBs purity can reduce expensive purification steps after refolding. [71] Solubilization of the IBs and refolding of the solubilized proteins are the major challenges. [61] Traditionally, high concentrations of urea and guanidine hydrochloride have been used to solubilize the IBs. If the recombinant protein also has disulfide bonds, additional reducing agents that reduce possible disulfide bonds are needed for solubilization. For example, beta mercaptoethanol, dithiothreitol,[71] or tris(2-carboxyethyl)phosphine (TCEP) are suitable for this purpose.[38] The use of highly chaotropic compounds in solubilization destroys all protein structures. In some cases, this can also lead to protein aggregation. Therefore, milder solubilization conditions that preserve secondary structures can be used as an alternative. After the protein has been solubilized, it must be folded into its natural structure.[71] To allow this, the reagents used for solubilization must be removed. The most common methods for this are diluting the solubilisate into refolding buffer [33] or dialyzing the solubilisate against refolding buffer.[79] However, these methods have the disadvantage of requiring a large amount of buffer and showing low refolding yield, due to protein aggregation. Low intermolecular interactions and low protein concentrations counteract this aggregation and are therefore a requirement to increase refolding yield. [71] For example, arginine in the refolding buffer leads to a reduction in protein-protein interactions. [61]

1.5 Role of oxidation reduction potential and oxygen

Oxidation reduction potential (ORP) reactions occupy a significant position within biological processes. These chemical reactions are involved in diverse regulatory mechanisms, including energy metabolism, respiration, photosynthesis, gene expression, signal transduction, protein folding, and disulfide bond formation. [51] Disulfide bonds can be involved in protein stability, activity and folding. These are formed from two cysteines and an oxidation reaction in which two electrons are removed from the protein. The counter reaction to this would be a reduction reaction in which the disulfide bond is broken and the protein accepts two electrons.[51, 6] The importance of the redox potential as a culture variable is already well known for native folding of proteins in cells. In the field of protein refolding, it is assumed that at the later stage, an oxidative redox potential enhances protein folding and disulfide bond formation. Furthermore,

it has been shown in cells that an appropriate balance between reductive and oxidative species optimizes the oxidative folding of several proteins. [53] The use of air or oxygen can support protein refolding from dissolved protein solutions. This approach has proven effective, for example, in the refolding of prochymosin, where the oxygen supply was tightly regulated and redox couplings were used. Under these conditions, improved reactivity and restoration of the correct protein structure were observed.[54] Thus, targeted control of the redox environment and optimized oxygen supply represent promising approaches to support the refolding process of proteins.[53] There are two main systems in the literature for promoting disulfide bond formation *in vivo*: the oxido-shuffling system and oxygen-mediated oxidation. The oxido-shuffling system is a redox system consisting of an oxidized and a reduced form in 1:1 to 1:10 ratio. This system supports the formation of disulfide bonds. Well-known representatives of this system are glutathione (GSH/GSSG), cystine/cysteine and cystamine/cysteamine. All these representatives share the same mechanism and consist of a low molecular weight thiol (LMW thiol) and a low molecular weight disulfide (LMW disulfid). The mechanism is ultimately based on a thiol-disulfide exchange reaction, which occurs through two nucleophilic attacks of a thiolate anion. The second method mentioned is based on oxygen or air, which is used as an oxidant in this case. It is assumed that this occurs via the formation of cysteine bonds in this case via the formation of cysteine sulfenic acid. This method is relatively favorable, since the oxygen can be supplied via air. However, the kinetic is slow and the upscaling is difficult with the oxygen mediated method. [53, 15]

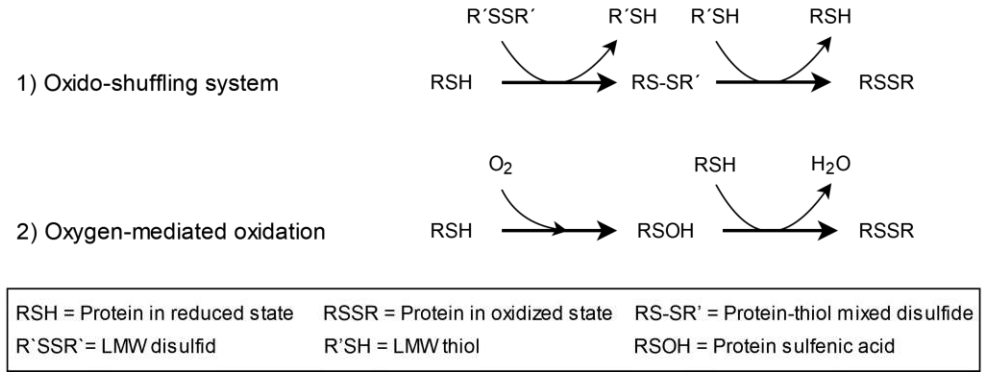

Figure 1.1: Reaction scheme for the formation of disulfide bonds during protein refolding. Point one shows oxido-shuffling systems and point two shows oxygen mediated systems.[12]

To change the concentration of DO in a solution, air or oxygen in the form of bubbles is often simply introduced into it.[15, 53] However, problems can arise if proteins are present in the solution, as both the bubbles themselves and the resulting foam can affect the protein. Proteins show a strong affinity for gas/water interfaces and can be adsorbed there.[87] This absorption stabilizes the bubble lamellae in the foam by locally

reducing surface tension and creating stress gradients at the surface that counteract membrane thinning. Furthermore, proteins can form cohesive films at the interface and form extensive intermolecular interactions. [21, 83] In addition, absorption results in conformational changes known as surface denaturation. These effects can lead to protein aggregations occurring, where both soluble and insoluble aggregates can form. For example, in the work of Yiming Xiao [87], a reduction in soluble protein concentration due to flow-through bubbles was observed. For this reason, DO should not be introduced into the solution via bubbles during refolding, as this could have negative effects on the protein.[21, 87] Possibilities for bubble free gassing of bioreactors are shown in figure 1.2 A frequently used method is gassing via the headspace or the surface. However, this method is mainly used for shake flask cultivations [88] and microtiter plates.[28] In this variant, the ratio between gassed surface and total volume plays an important role and is therefore often not suitable for larger volumes.[49] Another possibility is gassing via an external loop, in which the contents of the reactor are pumped into an external area where they are enriched with oxygen (for example by blowing in air) and then pumped back again. With this method, however, the critical factor must be separated before oxygen is added. In the case of cells, these would have to be separated beforehand.[49, 68] Another variant of bubble free gassing is via an oxygen-permeable membrane, which introduces oxygen into the reactor medium via diffusion. In this case, an oxygen-permeable membrane in the form of a tube is often used, which is inserted into the medium. This variant is often used for mammalian cell cultures.[68, 60]

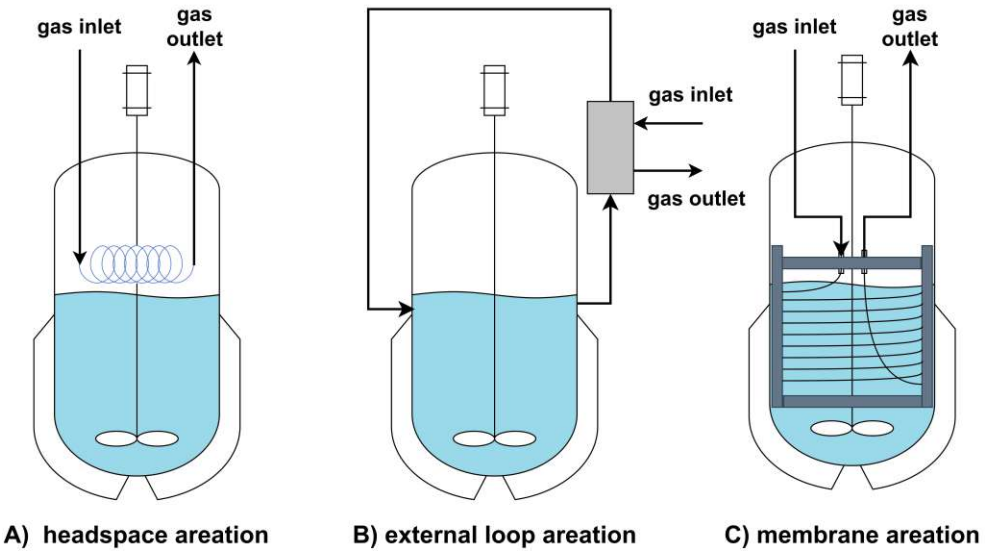

Figure 1.2: Schematic representation of three possible variants of bubble free gassing. Part A represents gassing via the headspace or the surface, part B via an external loop, and part C via an oxygen-permeable membrane.

To influence the redox potential during refolding, both oxidizing agents and reducing agents can be used. Since reducing agents are already used during the solubilization step in the presence of disulfide bonds, the redox potential is probably negative. To specifically change the redox potential during refolding, oxidizing agents such as molecular iodine, ferricyanide, tetrathionate and hydrogen peroxide can be found in the literature (*in vivo*), which can shift the redox potential into the positive range. [42]

1.6 Galactose oxidase

Galactose oxidase is a mononuclear copper enzyme.[40] In past times, the origin of galactose oxidase (GalOx) was thought to be *Polyporus circinatus*. Later, the assumption was transferred to *Dactyliumdendroides*. Nowadays, however, it is assumed to be derived from the genus *Gibberella* (*Fusarium*).[34] Galactose oxidase represents a remarkable copper enzyme that catalyzes the two-electron oxidation of a considerable number of primary alcohols to corresponding aldehydes and reducing oxygen to hydrogen peroxide. In the case of galactose, this leads to the formation of D-galacto-hexodialdose as well as hydrogen peroxide. The enzyme exists in monomeric form and consists of an amino acid sequence with a total of 680 amino acids. It has a molar mass of approximately 72.823 kDa and possesses two disulfide bonds.[40, 34]

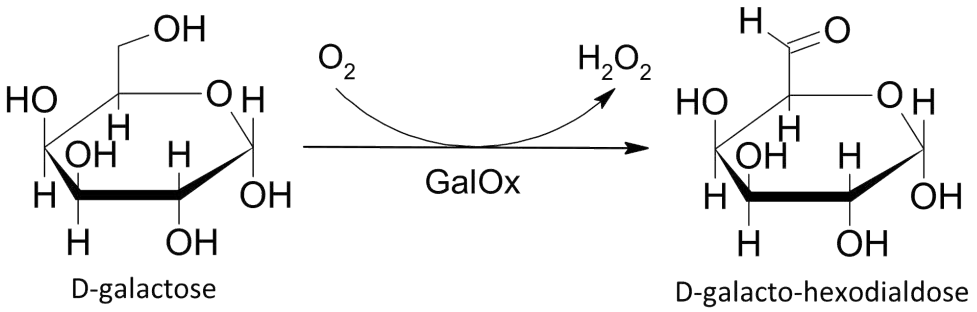

Figure 1.3: Schematic reaction equation of GalOx with the substrate galactose.[34]

Galactose oxidase is a metalloenzyme that binds a copper ion in a square-pyramidal coordination with two histidine ligands (His496, His581) and two tyrosine ligands (Tyr272, Tyr495). One of the tyrosine ligands (Tyr272) has a unique feature in that it forms a covalent cross-link with a cysteine (Cys228) on a carbon atom of the phenol ring. This creates a cysteinyl-tyrosine dimer in the active site, which is protected by a tryptophan (Trp290) residue that fits over it like a shield. This cysteinyl tyrosine dimer formation is an important post-translational modification required for enzyme activity. It can occur spontaneously when copper and oxygen are present.[7] In the literature it is also reported that this post-translational modification can also be formed without oxygen, in which case a different mechanism is used.[63] In addition, the cysteinyl

tyrosine dimer is redox active, which means that the enzyme has two redox centers: the protein itself and the metal center. This leads to three different oxidation states in the enzyme. The fully oxidized form contains a Cu^{+2} ion and a tyrosyl radical, the intermediate form contains a Cu^{+2} ion and a tyrosine, and the reduced form contains a Cu^{+1} ion and a tyrosine. Only the fully reduced and fully oxidized forms exhibit catalytic activity. The transition between these forms occurs via a two-electron redox step. The complex reduced with one electron shows no catalytic activity and is therefore inactive.[7]

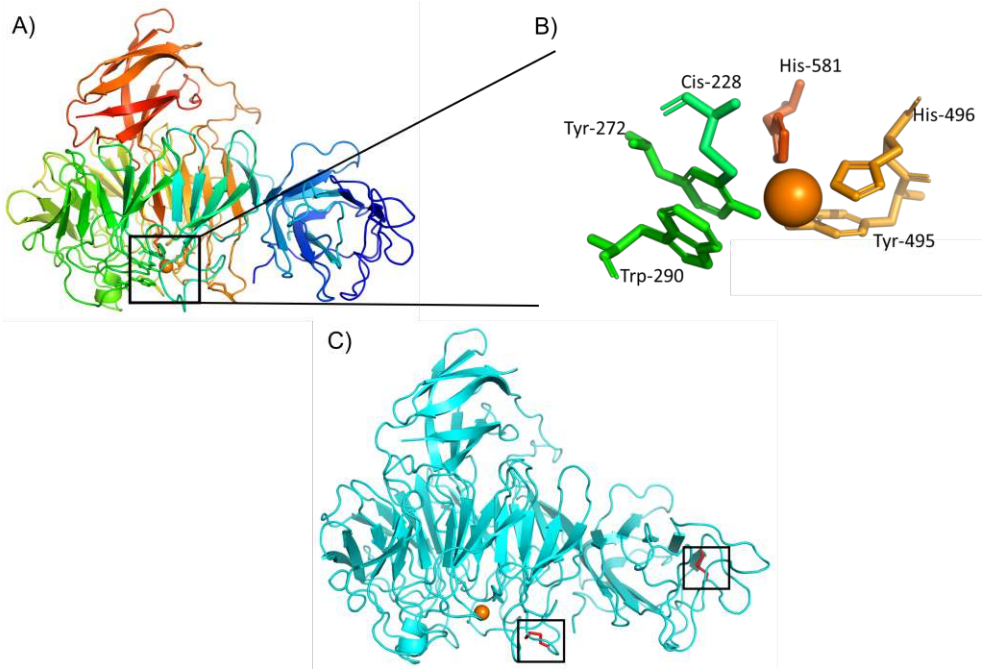

Figure 1.4: A) Graphical representation of the simulation of GalOx based on X-ray structure analyses. B) Graphical representation of the ligands of GalOx to the copper ion. The orange sphere represents the copper ion. C) Additional graphical simulation of GalOx with disulfide bonds.

Another aspect of GalOx is that it does not require an organic redox cofactor (like flavins, nicotinamide, ubiquinone) for hydrogen transfer during catalysis. Instead, it is able to accomplish this transfer via its copper complex.[84] In principle, GalOx offers a broad application potential as a biosensor. However, it is important to note that depending on the variant of the GalOx, different substrate spectra can be converted. Protein engineering has led to the development of variants that can also oxidize secondary alcohols. This allows, for example, biosensors to be developed that are specific for galactose as well as for a variety of sugars. This opens up possibilities for developing highly specific biosensors for different applications. Considering the analytical

sample, this can also be used for the detection of lactose in milk.[80] Furthermore, these can then also be used in medical diagnostics, for blood or urine.[65] In addition, it is possible to immobilize the GalOx on surfaces, which opens up further application possibilities. By immobilizing GalOx in a laponite clay film on a PT electrode surface, a versatile amperometric sensor that can be used in a variety of applications was developed. The GalOx can also be cross-linked to surfaces, for example, this was achieved with glutaraldehyde, which preserves its activity longer. Galactose oxidase has also found application in chemical syntheses. For example, it has been successfully used in the synthesis of 4-deoxy-D-glucose derivatives, dihydroxyacetone phosphate, and L-fructose There are also GalOx variants reported in the literature that exhibit high enantioselectivity toward a wide range of racemic chiral secondary alcohols, which accordingly enables enantioselective sensors.[80] The tensile strength and folding strength of paper can be improved by adding GalOx as an additive. This is done by oxidizing galactomannans, which modifies their structure.[25] Galactose oxidase can also be found in the field of cancer screening methods, for example, it can be used for the determination of galactose-N-acetyl-galactosamine, which is considered a cancer indicator.[69]

1.7 Quality by Design and Process Analytical Technology

Quality by Design (QbD), is a concept from the field of quality assurance, which was first used by Juran in 1985. It is used in many fields, such as pharmacy, automotive industry, food industry, etc. This concept is based on the idea that quality cannot be tested into a product, but must be planned into the development. In the pharmaceutical industry, the International Council for Harmonisation of Technical Requirements for Pharmaceuticals for Human Use (ICH) guidelines Q8-12 deal with this issue.[67] Two important points in QbD are critical quality attributes (CQA) and critical process parameters (CPP). According to the ICH Q8 (R2), CQA is a physical, chemical, biological, or microbiological attribute or characteristic that provides the desired product quality within a certain range, limit, or distribution. CPPs are also defined in ICH Q8 (R2) as process parameters whose variability has an impact on CQA and therefore must be monitored or controlled to ensure that the process provides the desired quality. Ideally, CPPs should be mechanistically linked to CQAs.[75] An important tool of QbD is Process Analytical Technology (PAT), this can be considered as a kind of toolbox and is therefore an important tool for a better process understanding, the definition of control strategies and for continuous improvement. Improving the control and understanding of the manufacturing process can be considered as a goal of PAT. It was originally introduced by the US Food and Drug Administration (FDA).[36] PAT is an analytical system rather than an analytical instrument that requires real-time data. The information can come from mathematical models, process analyzers, or from a laboratory test, but it must be real-time or near real-time data. PAT allows quality to be integrated into the product using the principles of QbD. Furthermore, it allows the control of CQAs directly or via CPPs and material CQAs, which have a direct influence on certain product CQAs.[67, 22]

1.8 Activity detection

The most commonly used method for determining the activity of GalOx is via the hydrogen peroxide formed in the reaction. Hydrogen peroxide, with the help of an oxidase such as Horseradish Peroxidase (HRP), can convert 2,2'-azino-bis(3-ethylbenzothiazoline-6-sulfonic acid) (ABTS), producing a radical cation that can be determined photometrically. As mentioned earlier, the use of hydrogen peroxide to adjust the redox potential can be found in the literature. However, this possibility of adjustment is not compatible with the ABTS assay since it is based on hydrogen peroxide. An alternative to the ABTS assay would be an assay based on 3-methoxybenzyl alcohol (3MBA). In this assay, the GalOx catalyzes the reaction to 3-methoxybenzylaldehyde, which has an absorbance at 314 nm. However, this assay is ten times less sensitive compared to the ABTS assay.[7]

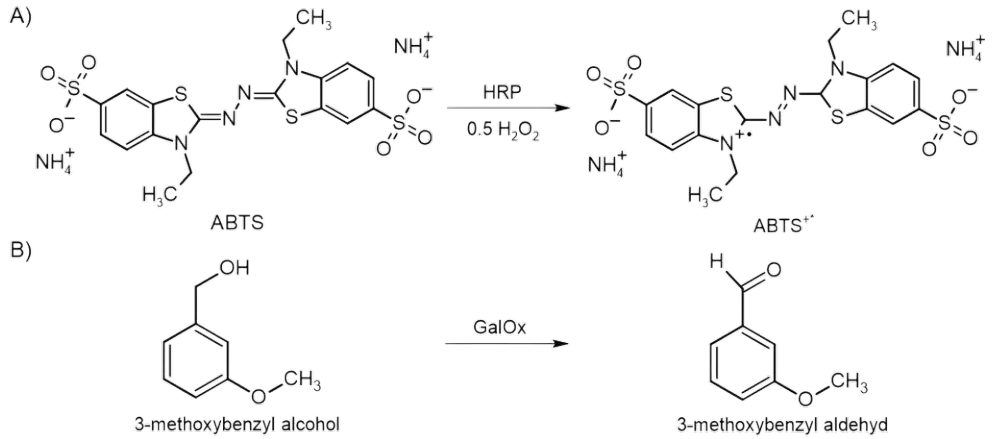

Figure 1.5: Schematic reaction diagram of the activity determinations of galactosexoidase with ABTS and 3MBA. Part A shows the activity determination with ABTS. The GalOx reduces galactose to D-galacto-hexodialdose. This produces H_2O_2 which, with ABTS, leads to the formation of a radical cation which can then be determined photometrically. Part B shows the activity determination with 3MBA, in which the GalOx oxidises 3-methoxybenzyl alcohol to 3-methoxybenzyl aldehyde, which can then be determined photometrically.[7]

1.9 Ellman's assay

The Ellman's assay is an analytical method for the determination of sulfhydryl groups (for example cysteamines, cysteine). This method is based on the reaction of the Ellman's reagent, which is 5,5-dithio-bis-(2-nitrobenzoic acid) (DTNB), with the sulfhydryl groups. This produces 2-nitro-5-thiobenzoates (TNB), which exhibit absorption at 412 nm.[4, 56]This reaction produces not only TNB, but also a so-called mixed disulfide. DTNB not only reacts with sulfhydryl groups, but can also react with TCEP, forming two TNB anions. A graphical representation of the reactions of DTNB with TCEP and sulfhydryl groups can be seen in figure 1.6.[38]

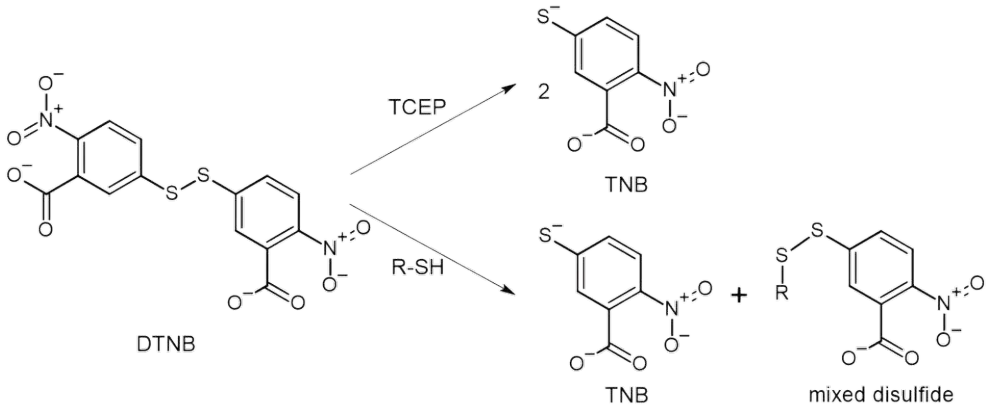

Figure 1.6: Schematic reaction of Ellman's reagent (DTNB) with TCEP and sulfhydryl groups.

1.10 Models

Models are often used in science to describe reality in a simplified way. [74] Models help to improve the process understanding and in the QbD guidelines it is also recommended to link the CPPs with the CQAs mechanistically.[67] There are different types of models, such as white box models or black box models. White box models like mechanistic models are based on basic physical principles, typically using simplified mathematical formulations of causal mechanisms. Black box models, on the other hand, are based on complicated mathematical operations (neural networks, decision trees, etc.), which are very difficult to explain and can only be understood by very few experts. Blackbox models are based on an input-output relationship, which has to be created over large amounts of data.[52, 5] . To build white box models, data is also needed. Often relatively simple differential equations are provided with model parameters. If a white box model is projected onto protein refolding, the differential equations describe the mechanism and the model parameters describe the reaction rate constants. [58] A variety of mechanisms dealing with protein refolding can be found in

the literature.[23, 29, 44, 47, 90, 66] These have most similarity to the three classical models of Dill and Chan[26] shown in figure 1.7. The models are based on solubilized protein, folding intermediates, and the native protein. Currently, it is assumed that the reaction from solubilized protein to folding intermediates is instantaneous .[39]. Furthermore, it is currently also assumed that the formation to the native protein occurs via a first order reaction. All other reaction mechanisms can be first, second or third-order [29, 39, 47, 90, 57].

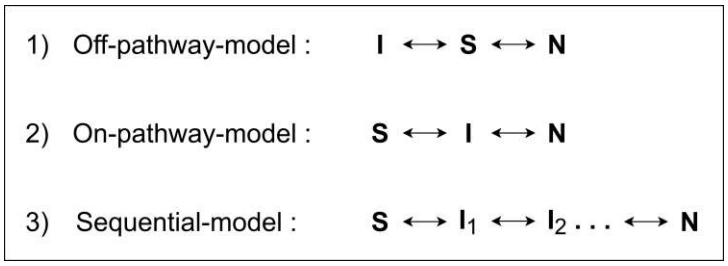

Figure 1.7: Dill and Chan's three classic models of the behavior of proteins during refolding. S stands for solubilized protein, I for intermediate protein and N for native protein. [26]

1.11 Goals of this thesis

Protein refolding currently follows an empirical approach rather than a QbD approach. In industry, only low refolding yields of 15-25 % are achieved and PAT tools in protein refolding are rare. However, QbD and PAT are state-of-the-art in the pharmaceutical industry and allow gathering of process understanding, process control and risk-based decision making. The identification of new PAT tools for protein refolding is therefore a relevant factor for the future to improve refolding yields and process understanding. Another challenge in the field of protein refolding is the handling of posttranslational modificaktion (PTMs) such as disulfide bonds. These are reported to be present in around 18 % of human proteins and in all biosimilars recently approved (2021-2022) for the EU market. A potential candidate as CPP is the redox potential, since the formation of disulfide bonds takes place via a redox reaction and since an influence of the redox potential in the area of folding has already been reported in the literature *in vivo*. Another potential candidate as CPP is DO, which on the one hand could lead to the formation of oxidation products, but can also support the formation of disulfide bonds. Furthermore, it also has an influence on the redox potential and could therefore possibly also serve as a cost-effective oxidant for a possible redox control strategy. The control of DO and redox potential via DO requires bubble free aeration methods, as air-water interfaces could bring several negative aspects. Furthermore, other suitable oxidants for GalOx should be found to study and control the influence of redox potential and DO more independently. To find out if the DO and/or the redox potential act as CPPs and can be used as a PAT tool, control strategies for the redox

potential and the DO need to be developed to perform refolding processes at different values of these parameters, and by mathematically linking these possible CPPs with the CQAs a PAT tool could then be developed. This will lead to the following key questions.

- Can the DO be controlled in a refolding process, and if so, what is the technical implementation and control strategy?
- How can the redox potential be controlled in a refolding process using DO, what is such a control strategy and are there alternative oxidants to control the redox potential?
- How does the redox potential or the DO influence the activity of the GalOx during refolding?
- Is it possible to establish a mathematical link between the activity and the DO and/or the redox potential, that can then be used for a potential model?

2 Materials and Methods

2.1 Software & Chemicals

2.1.1 Software

Table 2.1 contains a list of the programs used in the work. Furthermore, the version number of each program is given.

Table 2.1: List of used software.

Name	Version
Autodesk Fusion 360	2.0.15509
Chromeleon	7.2.10
Lucullus PIMS	03.11.2007
MODDE Pro	13.0.2.34314
PrusaSlicer	2.5.0
pyOptSparse	2.9.0
Python	3.9.12
Statsmodels	0.13.5
Tecan SPARKCONTROL	-
PyMol	2.5.5

2.1.2 Chemicals

The chemicals used for the experiments were mainly from Roth and Sigma-Aldrich. Table 2.2 lists the manufacturer, the corresponding cas number and the purity of the chemicals for each chemical used.

Table 2.2: List of used chemicals.

Name	Manufacturer	Cas-number	Purity
ABTS®Biochemica	PanReac AppliChem	30931-67-0	-
Aceton Rotisolv®HPLC	Roth	67-64-1	$\geq$ 99.9 %
Acetonitrile	PanReac AppliChem	75-05-08	99.9 %
L-Arginine	Roth	74-79-3	$\geq$ 98.5 %
Copper-(II)-sulfate	Roth	7758-98-7	$\geq$ 99 %
Cystamine dihydrochloride	Sigma-Aldrich	56-17-7	96 %
5,5´-Dithio-bis-(2-nitrobenzoesäure)	Roth	69-78-3	$\geq$ 98 %
Ethylenediamine tetraacetic acid disodium salt dihydrate	Roth	6381-92-9	$\geq$ 99 %
D(+)-Galactose	Roth	59-23-4	$\geq$ 98 %
Galactose Oxidase from Dactylium dendroides	Sigma-Aldrich	9028-79-9	-
Guanidine hydrochloride	Roth	50-01-1	$\geq$ 99.7 %
Hydrochloric acid 37 %	Roth	7647-01-0	-
Hydrogen peroxide 30 %	Fluka	7722-84-1	-
Iodine	Roth	7553-56-2	$\geq$ 98.5 %
3-Methoxybenzyl alcohol	Merck	6971-51-3	98 %
N2 (gas)	Messer	-	99.999 v %
O2 (gas)	Messer	-	99.999 v %
Peroxidase, Horseradish	Merck	9003-99-0	-
Potassium hexacyano-ferrate(III)	Merck	13746-66-2	99 %
Potassium tetrathionate	Sigma-Aldrich	13932-13-3	-
Potassium permanganate	Merck	-	99 %
Protein standard 2 mg BSA	Sigma-Aldrich	9048-46-8	$\geq$ 99 %
ROTI®Calipure pH4	Roth	-	-
ROTI®Calipure pH7	Roth	-	-
Redox standard 124 mV	Sigma-Aldrich	-	-
ROTI®Calipure 475 mV	Roth	-	-
Sodium dihydrogen phosphate monohydrate	Roth	231-449-2	$\geq$ 98 %

Sodium choride	Sigma-Aldrich	7647-14-5	$\geq$ 99.5 %
Sodium chlorate	Roth	7775-09-9	-
Trifluroacetic acid	Roth	200-929-3	$\geq$ 99.9 %
Tris Pufferan®	Roth	64431-96-5	$\geq$99.9 %
Tris-(2-carboxyethyl)-phosphin Hydrochlorid	Roth	-	$\geq$ 98 %
Tween® 80	Roth	9005-65-6	-
Sodium Hydroxide	PanReac AppliChem	1310-73-2	98 %

2.2 Inclusion budy preparation

2.2.1 Biomass & inclusion body isolation

The biomass containing the IBs was provided by a research group at the technical university of vienna. It was obtained via fermentation of an *E. coli* BL21 (DE3) strain with a T7 expression system and the GalOx gene of *Fusarium graminearum*. This organism was engineered at the Vienna University of Technology. Frozen biomass (*E. coli* with IBs) was resuspended in lysis buffer (100 mM Tris, 10 mM Na-EDTA in H_2O at pH 7.4) to a final concentration of 833 g wet weight L^{-1}. The resuspended cells were then homogenized using a GEA PandaPlus 2000 at 1200 bar. The cell suspension was considered to be homogenized after the solution had gone through three cycles. After the homogenization, the solution was centrifuged at 4° C. 13 000 g for 20 min. The supernatant was discarded and the pellet was resuspended in buffer A (50 mM Tris, 500 mM NaCl, 0.02 w % Tween 80 in H_2O at pH 8.0) to a concentration of 833 g wet weight L^{-1} . The resuspended solution was then centrifuged at 4 °C, 13 000 g for 20 min. The supernatant was discarded and the pellet was resuspended in buffer B (50 mM Tris, 5mM Na-EDTA in H_2O at pH 8.0) to a concentration of 100 g wet weight L^{-1}. The resuspended solution was then separated into Falcons (approximately 40 mL) and Eppendorf tubes (approximately 1 mL). Falcons were then centrifuged at 4 °C, 13 000 g for 20 min. Eppendorf tubes were centrifuged at 4° C at 20 000 g for 5 min. The supernatant of both was discarded. The mass of the pellet was determined and frozen at -20 °C until used for further experiments.

2.2.2 Inclusion body solubilization

Frozen IBs were resuspended with solubilization buffer (6 M GuHCL 0.15 M NaH_2PO_4 in H_2O at pH 7.0), using a concentration of 100 g L^{-1} of solubilization buffer. Then 25 µL 1 M TCEP (in H_2O) was added per mL solubilization buffer used. After the TCEP addition, the solution was only carefully homogenized. The mixture was incubated for 2 h on a shaker. Thereafter, the mixture was centrifuged at room temperature or 4 °C at 12 000 g for 15 min. The pellet was discarded and the supernatant was

transferred to a new tube and stored in the refrigerator or on ice. The solubilisate was freshly prepared.

2.3 Construction of a diffusion hose holder

For the development of a diffusion hose holder, 3D drawings were created in Fusion 360, these were then converted into a 3D print medium with the PrusaSlicer-2.5.0 and printed with a Prusa i3 MK3S. The outer diameter of the frame and the diameter for the hose bushings were determined using previously created print templates. The frame was printed modularly in order to be able to print the feedthroughs vertically. All components were printed with a nozzle temperature of 215 °C and a build plate temperature of 60 °C. 0.15 mm was used as the layer height. A minimum of two layers was set for the vertical contour skin and 4 layers for the horizontal contour skin. Adaptive cubic was used as infill, with a filling density of 40 %. The individually printed modules were cleaned of print residues and connected to each other with acetone. Prusament PLA (polylactic acid) Gentleman's Grey was used as the print material. Figure 3.1 shows a sketch of the created frame. In this, two larger holes can be seen at the top end, these serve as passages for two pass throughs, which couple the diffusion hose to the frame. A more detailed sketch is included in the appendix.

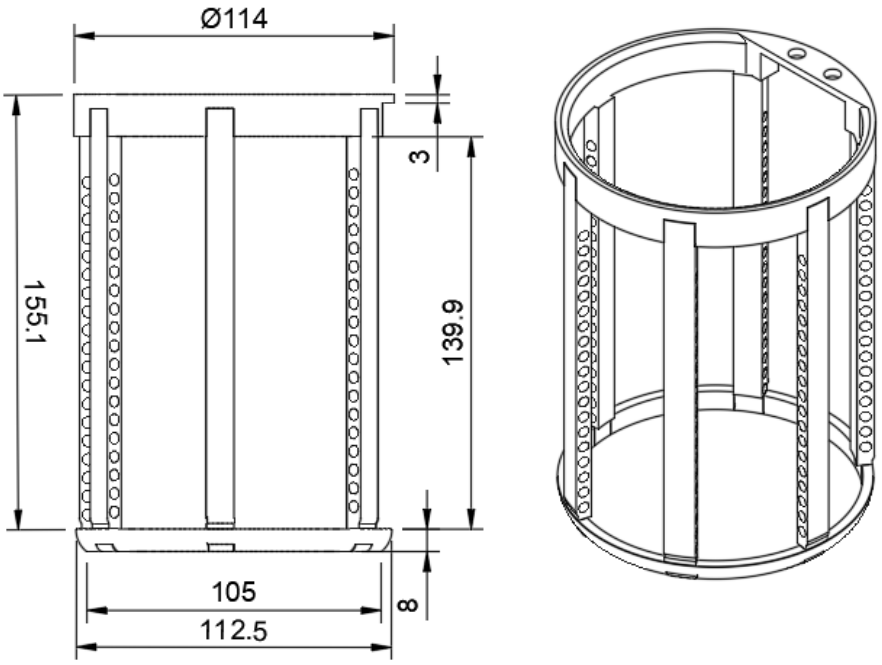

Figure 2.1: Sketch of the developed diffusion hose bracket, with the basic dimensions of the holder.

2.4 Workflow refolding reactor

2.4.1 Reactor setup

A 3.5 L glass reactor with a stainless steel lid and a double jacket was used as reactor. The reactor was controlled via a Labfors 4 Tower (Infors), which in turn was controlled via the Lucullus control software (Securcell). The internal PID controller of the Labfors 4 was used for pH control. For this purpose, 0.2 M or 0.8 M HCl was used as the acid and 0.5 M NaOH as the base. The temperature was controlled with a Lauda alpha RA 8, which was directly attached to the reactor jacket. A 6* blade stainless steel rushton turbine with a 48 V direct drive was used as the stirrer. An overpressure of 0.25 bar was set in the diffusion hose by regulating the outflow rate of the hose. A pH probe (Hamilton, EasyFerm Plus PHI K8 325), redox probe (Hamilton, EasyFerm Plus redox Arc 425), temperature probe and DO probe (Hamilton, VISIFERM DO 425) were mounted into the reactor for inline measurements. The aeration took place via a diffusion hose and via the head space. The mass flow controllers were connected to each other via two Y-pieces. A barometer was connected after the connecting pieces in order to be able to set or measure the pressure in the diffusion hose. After the barometer, the diffusion hose was connected, behind which a mechanical regulator was mounted to regulate the pressure in the diffusion hose. The gas then entered the headspace and then the exhaust air. Two ready-y mass flow controller (MFC) from Vögtlin (GSC-C3SA-BB26 and GSC-B59A-B26) and an OKS 4800 (4850ABC2H1B1K2C00A) from Brooks were used. Figure 2.2 shows a sketch of the gassing construction.

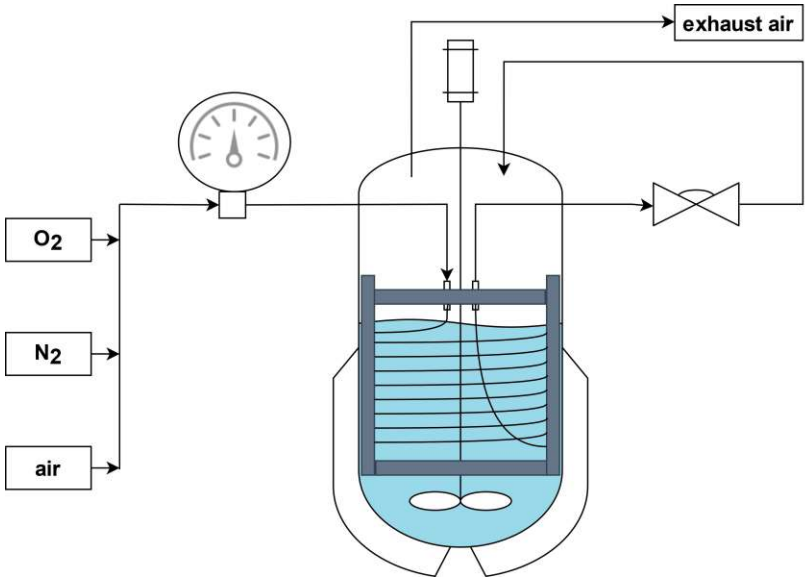

Figure 2.2: Sketch of the gassing system of the Reactor. Three MFCs (O_2, N_2, air) create a gas flow that goes into the diffusion tube and then into the headspace.

2.4.2 Reactor preparation

The pH electrode was calibrated with a pH 4 and pH 7 standard. The redox probe was calibrated with a 475 mV and 124 mV standard. 1 L refolding buffer (1 M Arginine, 0.1 M NaH_2PO_4, 1 mM Cystamine in H_2O at pH 7.4) was introduced into the reactor, the diffusion tube was placed in the reactor and all other components were connected to the reactor. A temperature of 10° C, a stirrer speed of 200 rpm and a pH value of 7.4 were then set. The DO probe was calibrated using N_2 and air.

2.4.3 Reactor refolding procedure

The controllers described in section 2.6 were applied and after the controlled value had stabilized, 25 mL of solubilisate (see section 2.2.2) were added into the reactor. A sample was then taken at regular intervals for at-line measurements. The activity of this was then determined via the ABTS assay (see section 2.10.2) and the protein concentration via the HPLC (see section 2.10.4). In certain runs, the Ellman's assay (section 2.10.1) was measured and the activity was determined using the 3MBA assay(see section 2.10.3. Furthermore, the temperature, the DO, the pH and the redox potential were measured inline. After about 24 h, a 1 M $CuSO_4$ solution was added to achieve a final concentration of 1 mM $CuSO_4$ in the reactor. The reactor run was terminated after 30 h at the latest.

2.4.4 List of reactor runs

Several reactor runs were carried out, in the table 2.3 a list with these is given. Furthermore, it is given which parameter was kept constant during which run.In total, 6 runs were performed at either constant DO or constant redox potential. The run at a DO of 0 was also used for the reactor runs at constant redox potential, as these run was at an almost constant redox potential of -300 mV.

Table 2.3: List of performed reactor runs, with the name of the run and the controlled parameter.

Name	Value kept constant
DO0/Redox-300	dissolved oxygen 0 %/ redox potential -300 mV
DO30	dissolved oxygen 30 %
DO80	dissolved oxygen 80 %
DO120	dissolved oxygen 120 %
Redox-200	redox potential -200 mV
Redox-150	redox potential -150 mV

´

2.5 $K_L a$-determination

For the determination of the oxygen mass transfer coefficient ($k_L a$), the same reactor setup as described in section 2.4 was used. The measurements were performed in refolding buffer. One series of measurements was performed with headspace gassing only, and another with headspace gassing and the difussion tube. The $k_L a$ was determined by fitting the measurement data to the formula 2.1.

$$\frac{\mathrm{d}DO}{\mathrm{d}t} = k_L a * (DO_{max} - DO_{mea}) \tag{2.1}$$

$\frac{\mathbf{d}DO}{\mathbf{d}t}$	$[\%h^{-1}]$	change in DO per time
$\boldsymbol{k_L a}$	$[h^{-1}]$	gas-liquid mass transfer coefficient
DO_{mea}	[%]	measured value of the DO
DO_{max}	[%]	maximum attainable DO (100)

2.6 Control strategies

2.6.1 Control strategy DO0

In order to achieve a target value of 0 % DO, N_2 was continuously introduced into the reactor at 1 L min^{-1}.

2.6.2 Control strategy DO30 & DO80

The same controller structure was used for the run at constant DO30 and DO80. PI controllers written in Matlab were used for this. Data was transferred via the Labfors 4 Tower, via lucullus, then to an Open Platform Communications (OPC) server and then to a corresponding computer on which the Matlab controller was running. The DO was controlled with air, whereby the output of the PI controller was limited to a maximum of 1 L min^{-1}. The P and I components used are listed in Table 2.4.

Table 2.4: Specification of the P and I components of the PI controller for the DO30 and DO80 run.

run	P	I
DO30	0.003	0.9
DO80	0.0072	1.1

2.6.3 Control strategy DO120

The controller to control 120 % DO was written in the lucullus software. With these, the DO regulation takes place via the control of the duration of O_2 shifts. The control consisted of three different control cycles, after each control cycle the measured DO determined the subsequent control cycle. The principle of the main control cycle is shown graphically in figure 2.3.

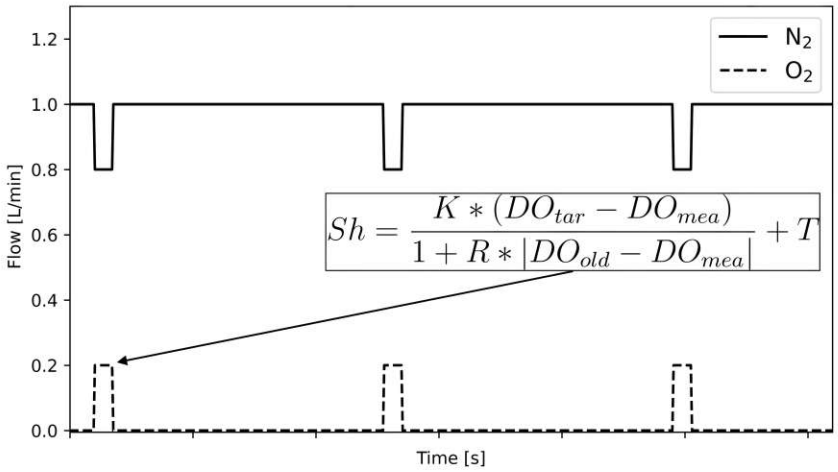

Figure 2.3: Schematic representation of the O_2 shift intervals. The dashed line represents the O_2 flow and the continuous line the N_2 flow. An increase in the O_2 flow always causes a decrease in the N2 flow, so that a flow of 1 L min^{-1} always occurs. The mathematical relationship for the duration of the shifts is given as a formula in the figure.

Sh	$[s]$	duration of the O_2 shift
DO_{tar}	[%]	DO set point
DO_{mea}	[%]	measured value of the DO (120)
DO_{old}	[%]	measured value of the DO of last cycle
K	$[s]$	control parameters (2)
R	[–]	control parameters (0.03)
T	$[s]$	control parameters (15)

If the measured DO was below 80 % of the set point at the end of a cycle, then 1 L min^{-1} O_2 was injected for 80 s. This O_2 shift was followed by gassing with 1 L min^{-1} N_2 for 220s. If the measured DO was 2 % above the target value at the end

of a regulation cycle, then N_2 was gassed with 1 L min^{-1} for 60 s. If the measured DO was between these two values (greater than 80 % and smaller than 102 % of the target value), then the regulation took place with 0.2 L min^{-1} O_2 shifts. Between these shifts, gassing was carried out with 1 L min^{-1} N_2 for 220 s and during these O_2 shifts an additional 0.8 L min^{-1} N_2 was used for gassing. Figure 2.3 shows a schematic representation of this control cycle sequence and the used equation for the control. The O_2 shift intervals resulted according to the formula in figure 2.3. The control variables K, T and R were empirically determined for the target value of 120 % DO.

2.6.4 Control strategy Redox-200

The redox control took place via the gassing of O_2 and N_2. Gassing with N_2 (N_2 step) was carried out above the target value and PI-controlled gassing with O_2 and N_2 (O_2 step) below the target value. In the O_2 step, there was a PI controller with a P component of 0.1 and an I component of 0.1, which regulated the O_2 component of the gassing. The control range of the PI controller was 0.15-1 L min^{-1} O_2. The gassing in this step was kept constant at 1 L min^{-1} with N_2. Manual was increased to 80 % DO before adding the solubilisate to the DO. The described controller was written in the Lucullus operations software.

2.6.5 Control strategy Redox-150

This controller was written in the operation tool from Lucullus. It has a DO pre control, which regulates the DO before the solubilizer addition (DO_{start}). The control is based on alternating O_2 and N_2 shifts. After this pre-control, three control cycles are connected in sequence, which control with decreasing oxygen content. These control cycles are always composed of two different steps, an O_2-containing step and an N_2 step. The transition from one control cycle to the next depends on the measured DO. The controller described here always uses a gassing rate of 2 L min^{-1} in total. The DO pre control is composed of a linear function (see equation 2.2) and a logarithmic function (see equation 2.3). The linear function determined a DO value (DO_{start}) from the redox set point, this function was created from the data of the DO runs and the Redox-200 run. The logarytmic function determined the duration of N_2 gassing between 30 s O_2 shifts to achieve the calculated DO_{start} value. The logarytmic function was created from empirical data. The transition from pre-control to the three sequential control loops occurred when the measured redox fell below 90 % of the redox set point.

$$Redox_{tar} = k * DO_{start} - d \tag{2.2}$$

$$DO_{start} = a * ln(N_2) + b \tag{2.3}$$

$Redox_{tar}$	$[mV]$	set redox set point
DO_{start}	[%]	target DO value befor solubilisate addition
k	$[mV\%^{-1}]$	model parameters (0.7085)
d	$[mV]$	model parameters (-283.32)
N_2	$[s]$	duration N_2 shift
a	$[-]$	model parameters (-97.88)
b	[%]	model parameters(563.16)

When the measured redox potential had fallen below 90 % of the redox set point, the first control loop of the redox controller started. This works with an O_2 step and an N_2 step. If the measured redox potential was lower than the redox set point, then O_2 was added with a PI controller. The PI controller regulated between 0.2 and 2 L min^{-1} O_2. With N_2, the total aeration rate was always kept at 2 L min^{-1}. The PI controller had a P component of 0.1 and an I component of 0.1. If the measured redox potential was greater than the redox set point, then N_2 was added at 2 L min^{-1}. When the measured DO fell below 90 %, the second control loop started. This gassed with 2 L min^{-1} air when the measured redox value was below the redox set point and with 2 L min^{-1} N_2 when the measured redox value was above the redox set point. As soon as the measured DO reached below 40 %, the third control circle started, which was set up in the same way as the second control circle, but instead of pure air, it used a mixture of 1.6 L min^{-1} air and 0.4 L min^{-1} N_2 when the measured redox potential was lower than the redox set point.

2.7 Screening for possible oxidation agents

40 mL of refolding buffer was pipetted into a beaker placed on ice and a previously calibrated pH electrode and redox electrode were placed inside. 1 mL of solubilisate (for preparation see section 2.2.2) was added and a sample was drawn. The oxidizing agent to be tested was then added step by step until a change in the redox potential was noticeable. Another sample was taken. The oxidant was then added again and another sample was taken. If the oxidizing agent did not cause any change in the redox potential, then only two samples were taken. From the samples which were taken, the activity was determined according to the section 2.10.2. In experiments with H_2O_2, the 3MBA assay(see section 2.10.3) was carried out in addition to the ABTS assay.

2.8 DoE time of copper addition & copper concentration

A Design of Experiment (DoE) was carried out with the factors time of copper addition and copper concentration. The experiment design is carried out with MODDE with a D-optimal design. The experiments resulting from the DoE are listed in tabular form and shown graphically in figure 2.5. Of the copper concentrations listed in figure 2.5, 100 x stocks were prepared with $CuSO_4$. Solubilisate was prepared according to section 2.2.2. 1 mL solubilisate was mixed with 40 mL cold refolding buffer. 990 µL of this mixture was placed in 27 eppendorf tubes. 10 µL of the corresponding 100 x $CuSO_4$ stock was pipetted according to the time data in figure 2.5. These refolding preparations were stored on a shaker at 4 °C before the addition of copper and after the addition of copper. After 3 h, the activity was analysed according to section 2.10.2 and the protein concentration according to section 2.10.4.

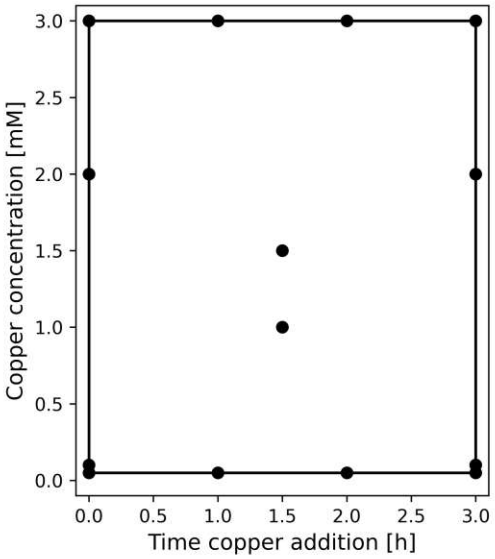

Reps	Cu [mM]	Time Cu addition [h]
2	0.05	0
2	0.1	0
1	2	0
2	3	0
2	0.05	1
1	3	1
1	1	1.5
4	1.5	1.5
1	0.05	2
2	3	2
3	0.05	3
2	0.1	3
2	2	3
2	3	3

Table 2.5: The figure shows the space covered by the DoE. The table includes the number of replicates performed under the same condition (Reps), the copper concentration used and the time at which the copper was added.

2.9 Basic characterisation 3MBA assay

The response of the GalOx catalysed reaction of 3-methoxybenzyl alcohol to 3-methoxybenzyl aldehyde was characterised. A Tecan Sparks plate reader with 96 well plates Greiner UV-Star F-botton was used for this purpose. All measurements were carried out at 30 °C. The different solutions with 3MBA and the GalOx standard were prepared with a 0.1 M NaH_2PO_4 buffer at pH 7.4. A prepared Galox solution was centrifuged at 4 °C 12 000 g for 5 min before use. A wavelength scan was performed to characterise the absorbance. For this purpose, 50 µL of 1 g L^{-1} GalOx standard was mixed with 150 µL of a 60 mM 3MBA solution, incubated for 10 min at room temperature and a wavelength scan was recorded. The influence of the 3MBA concentration was investigated by mixing 50 µL 1 g L^{-1} GalOx standard with 150 µL 3MBA solution and measuring the absorbance time-dependently at 312 nm. For this purpose, measurements were performed with 60 mM, 100 mM, 150 mM and 200 mM 3MBA solutions. Then the influence of the ratio between 3MBA solution and GalOx standard was investigated. For this, a 1 g L^{-1} Galox standard was mixed with a 150 mM 3MBA solution in different ratios and the absorbance was measured time-dependently at 312 nm. A total volume of 300 µL was used. To analyse the influence of decreasing activity or increasing activity, 200 µL of 150 mM 3MBA solution was mixed with 100 µL of different Galox standards (0.01 g L^{-1} - 2 g L^{-1}) and time-dependent absorbance at 314 nm was determined. The measurements with the different Galox standards were additionally carried out with the ABTS assay (see section 2.10.2) in order to be able to compare the 3MBA assay with the ABTS assay. Measurements with the GalOx standards were not incubated with copper.

2.10 Analytical methods

2.10.1 Ellman's assay

50 µL sample/blank were mixed with 50 µL Ellman's reagent (0.1 M DTNB (5,5'-dithiobis-2-nitrobenzoic acid) in acetone). The mixture was incubated on a shaker at room temperature for 15 min. Thereafter, 20 µL of this mixture were diluted with 180 µL of Ellman's buffer (0.1 M NaH_2PO_4, 1 mM Na-EDTA in H_2O at pH 8.0). 40 µL of this were placed in three wells of a 96 well plate. 160 µL Ellman's buffer was pipetted into each well. This was followed by an absorbance measurement at 412 nm and 30 °C. The samples were determined as duplicates. As a blank, refolding buffer used (1 M Arginine, 0.1 M NaH_2PO_4, 1 mM Cystamine in H_2O at pH 7.4). A TECAN Spark microplate reader with 96 well plates Greiner polysterene F-botton was used for the absorbance measurement. The conversion of the determined absorbances to a TCEP concentration was carried out using a linear calibration line drawn up on the same day. Refolding buffer was used to create the calibration line.

2.10.2 ABTS assay

0.1 mL of HRP stock (0.6 g L^{-1} HRP in 50 mM Tris , 1 M $(NH_4)_2SO_4$ at pH 7.5) was combined with 2.4 mL of ABTS solution (6.125 g L^{-1} ABTS in 0.1 M NaH_2PO_4 at pH 7.5). Then, 13.33 v% of this ABTS/HRP solution was combined with 40 v% D-galactose solution (1 M D-galactose in 0.1 M NaH_2PO_4 at pH 7.5). To refolding samples, a 0.1 M $CuSO_4$ solution was added to a final concentration of 1 mM $CuSO_4$. This was not done if the samples already contained copper. This sample was then incubated for 30 min at 4 °C on a shaker and then centrifuged at 4 °C and 12 000 g for 5 min. The supernatant was then used for analysis. From the centrifuged sample, 50 µL samples were pipetted into three wells. Immediately before the measurement, 150 µL of master mix were added. This was followed by a time-dependent absorption measurement over 5 minutes at 420 nm and 30 °C. The samples were determined in duplicate. Refolding buffer (1 M Arginine, 0.1 M NaH_2PO_4, 1 mM Cystamine in H_2O at pH 7.4) was used as a blank. A TECAN Spark microplate reader with 96 well plates Greiner polysterene F-botton was used for the absorbance measurement. The master mix was stored in the dark on ice or in the fridge and used for up to two days. $\Delta A\ min^{-1}$ was determined from the time-dependent absorption measurement. For this purpose, the R^2 was determined for the first 5 measuring points. Then the R^2 value was calculated with one more measuring point. If the added measurement point increased the R^2 value, then another measurement point was included. This was repeated until there was no further increase in the R^2 value. The gradient was then calculated from these measurement points and used in the following formula to obtain U mL^{-1}.

$$\frac{U}{mL} = \frac{V_{total} * \frac{\Delta A}{min} * dilution}{V_{sample} * d * \epsilon * j} \tag{2.4}$$

V_{total}	$[mL]$	volume of the sample (0.05)
$\frac{\Delta A}{min}$	$[min^{-1}]$	change in absorbance per minute
$dilution$	$[-]$	dilution factor of the sample
V_{sample}	$[mL]$	total volume in the well (0.2)
d	$[cm]$	pathlength , calculated as truncated cone (0.5712)
ϵ	$[mM^{-1}cm^{-1}]$	extinction coefficient at 420 nm (36)[46]
j	$[-]$	conversions factor(1 mol H_2O_2 to 2 mol ABTS)[20]

2.10.3 3MBA assay

Copper incubation and subsequent centrifugation was performed on refolding samples in the same way as described in section 2.10.2. 100 µL of the copper incubated and centrifuged refolding samples were pipetted into three wells. 200 µL of a 3MBA-solution (0.373 mL 3MBA with 19.627 mL 0.1 M NaH_2PO_4 pH 7.5) was added and the absorbance was measured over 5 min at 314 nm and 30 °C. Samples were always determined in duplicate. Refolding buffer (1 M Arginine, 0.1 M NaH_2PO_4, 1 mM Cystamine in H_2O atpH 7.4) was used as a blank. A TECAN Spark microplate reader with 96 well plates Greiner UV-Star F-botton was used for the absorbance measurement. The R^2 was then calculated from the time-dependent absorption measurement in a 10 measurement point window. The slope was then calculated from the window with the highest R^2. This was then used in the subsequent calculation to get U mL^{-1}.

$$\frac{U}{mL} = \frac{V_{total} * \frac{\Delta A}{min} * dilution}{V_{sample} * d * \epsilon} \tag{2.5}$$

V_{total}	$[mL]$	volume of the sample (0.1)
$\frac{\Delta A}{min}$	$[min^{-1}]$	change in absorbance per minute
$dilution$	$[-]$	dilution factor of the sample
V_{sample}	$[mL]$	total volume in the well (0.3)
d	$[cm]$	pathlength , calculated as truncated cone (0.8332)
ϵ	$[mM^{-1}cm^{-1}]$	extinction coefficient at 314 nm (2.691)[77]

2.10.4 Determination of protein concentration

The protein was determined using an reversed phase high performance liquid chromatography (RP-HPLC) measurement, in which the absorption was measured at 280 nm, 260 nm, 214 nm and 412 nm. A Thermo Fischer Ultimate 3000 HPLC with a BioResolve column (RP mAb polyphenyl, 450 Å, 2.7 µm, 3.0 x 100 mm) was used for this. MQ with 0.1 v% TFA was used as mobile phase A and ACN with 0.1 v% TFA was used as mobile phase B. Before the TFA was added, the respective mobile phase was degassed in an ultrasonic bath for 30 min. The HPLC was operated at a flow rate of 0.4 mL min^{-1} and a column temperature of 70 °C. The gradient used is given in table 2.6.[48]

Table 2.6: Used gradient of the RP-HPLC.

Time [min]	Phase A [%]	Phase B [%]
0.0-13.5	75-25	25-75
13.5-15.5	25	75
15.5-15.51	25-75	75-25
15.51-20.5	75	25

For protein concentration determination, the total absorbance area at 280 nm from 4-12 min was used. This area was related to a protein concentration via a previously generated BSA calibration curve. For the linear calibration curve, five standards were measured with a concentration of 0.05, 0.1, 0.2, 0.5, and 1 g L^{-1} BSA.

2.11 Modeling

Within the parameterization processes, the specific activity was used as a central reference value. Here, the specific activity was calculated by dividing the volumetric activity by the average of all protein measurements of the corresponding run. For the parameterization of the models, the Python library "pyOptSparse" was used, specifically the optimizer named "CONMIN" (CONstrained function MINimization) was used. This optimizer is based on gradients and uses feasible directions to obtain efficient solutions.[24] The parameterizations were performed in iterative loops that were executed repeatedly. During these loops, different random starting values were used for each of the model parameters. The parameterization with the lowest squared error was used for further operations. Only four reactor runs were used for parameterization (see table 2.7).

Table 2.7: Reactor runs used for the parameterization of a possible model.

Name	Value kept constant
DO0/Redox-300	dissolved oxygen 0 %/ redox potential -300 mV
DO80	dissolved oxygen 80 %
DO120	dissolved oxygen 120 %
Redox-150	redox potential -150 mV

After optimization of the parameters, the mean square error (MSE) and root mean square error (RMSE) for all reactor runs were calculated with the obtained optimized parameters. The recorded redox potential and DO values were inserted into the differential equation as constants for each minute (except for base models). Furthermore,

the DO was used in the form of mM and the redox potential in the form of mV. Since reciprocal values of the DO were also tested in modeling try, all DO values were corrected and added by 0.1 % to avoid division by 0. To the sampling times of the samples 0.5 h were added, because after sampling a 30 min copper incubation followed. The protein concentration of the respective runs was used as initial values. As a basis for the parameterizations, a slight modification of the one pathway model from point 1.10 was used (see figure 1.7). The solubilization was neglected.

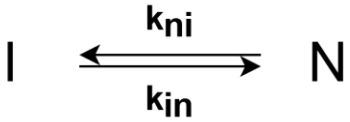

Figure 2.4: Kinetic model used for parameterization. k_{in} corresponds to the formation rate of the native protein (N) and k_{ni} corresponds to the degradation rate of the native protein. I stands for folding intermediate.

First, three basic models were parameterized, for each of which 25 individual optimizations were performed. These base models did not contain any parameter that changed over time or they were three constants. These included a model parameter for the formation reaction, a model parameter for the reverse reaction and a proportionality constant with which the formed native protein was converted to U g^{-1}. These three base models differ only in the reaction order of the back reaction k_{ni}. Base model one was based on a first order backreaction, base model two on a second order backreaction, and base model three on a third-order backreaction. For all parameterizations, the optimizer was given a space from 0 to 200 to optimize, with the inclusion of the proportionality constants, this was given a space from 0 to 10 000. A pool of variants of the DO and the redox potential were then generated. This contained the DO and the redox potential directly, their reciprocals, the quadratic form and the reciprocal of the quadratic form. Of all these forms, the exponential function was also included, and of all these variations, the negative form. This gives a number of 32 mathematical variants of the DO and the redox potential. The permutations from this pool were then used additively with a multiplicative model parameter in k_{in} and k_{ni}. This generated three times 930 models. In these extended models, the previously optimized basic model parameters were inserted as a number and consequently two model parameters were optimized for the parameterization of the extended models. The optimization was done over 10 loops with CONMIN. The same took place then again multiplicatively, then the mathematical variants from the pool with a model parameter were multiplicatively appended to the basic models. With the three best variants from the 6 kinetics variants, all model parameters were parameterized simultaneously, whereby the space for the parameters was set in the order of magnitude in which they were previously determined. This was followed by another 25 parameterization trials with CONMIN.

3 Results and Discussion

3.1 Development of bubble free gassing

3.1.1 Bubble free areation

In order to enable bubble free gassing, the possibilities mentioned in point 1.5 were examined in more detail. Gassing via a bypass was considered to be too complex, as the protein would have to be separated before gassing. Headspace gassing and membrane gassing were considered to be effective methods for efficiently changing the DO without bubbles. The headspace method is easier to implement than membrane gassing, since hardly any additional equipment is required. However, with the headspace variant, the diffusion surface for the oxygen is limited and a change in the DO is therefore probably only possible slowly. In order to enable bubble free gassing via a membrane, a holder had to be developed that allowed simple placement of a diffusion tube in the reactor. Figure 3.1 shows the developed holder.

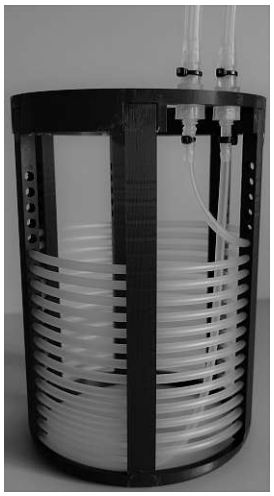

Figure 3.1: Photo of the diffusion tube holder printed from PLA.(the diffusion tube, the diffusion tube holder and the decoupling for the diffusion tube holder)

For the development of such a holder, several factors had to be considered, such as the lack of space in the reactor for the holder due to the reactor geometry and the components placed in the reactor (electrodes, stirrer, sample tube). Another problem

for the holder was that the wall thickness of the diffusion tube was thin and easily bent, which could lead to blockages in the tube. Furthermore, the material thickness of the holder had to be chosen carefully, since thinner wall thicknesses could save space in the reactor, but the risk of breakage of the holder during removal and installation would be problematic with a wall thickness that was too thin. The exact dimensions are shown in a figure included in the appendix. The diffusion tube was decoupled via a pass though on the rack, which reduced the mechanical stress on the diffusion tube during installation and removal. This also prevented kinking of the hose during installation, which would lead to increased pressure in the diffusion hose. (see figure 5.1) As already mentioned, the headspace variant for bubble free gassing was not considered sufficient to change the DO in a short time. Therefore, a frame was developed to place a membrane tube in the reactor. In order to show improvement with the diffusion tube experimentally, the $K_L a$ was determined once with the headspace gassing only and another time with the headspace gassing and with the diffusion tube. The resulting data are shown in table 3.1. It can be seen that the addition of the membrane gassing increased the $K_L a$ by more than 600 %, which should allow a much faster regulation of the DO. It should also be mentioned that the $K_L a$ values given, are many times lower compared to aeration methods with air bubbles.[35] However, by further increasing the membrane area, it should be possible to further improve the $K_L a$ via a bubble free gassing method.

Table 3.1: Determined $K_L a$ for headspace gassing and for headspace gassing in combination with the diffusion hose.

Aeration	$K_L a$ [h^{-1}]
Headspace	0.24
Headspace + Hose	1.78

3.2 DO and DO based redox controller

3.2.1 DO controlled reactor runs

With the developed gassing strategy and the developed DO control strategies, four reactor refolding runs were performed. A list is given in table 2.3. The run of the controlled DO is shown in figure 3.2. It should be mentioned here that the control strategy for the controlled DO was continuously developed. Consequently, the control strategy of the last run was more mature than that of the first run. Furthermore, control strategies must always take into account the factor that an overpressure in the diffusion chamber is needed to effectively influence the DO. The DO30 run was the first, in which several spikes can be seen, which were due to the PI control. After that the DO0 run took place, which was based on a gassing of 1 L min^{-1} N_2. This was followed by the DO80 run, which also exhibited spikes. However, these spikes were more

pronounced in the DO80 run, which was probably due to the higher P and I content of the controller. Furthermore, stronger fluctuations occurred after approximately 9 h with the DO80 run. The exact reason for this is not known. Comparing the DO30 run and the DO80 run, it can be seen that for the DO80 run the fluctuations around the set point were higher. Based on this controller, a DO120 run with O_2 and air was also attempted, which is not shown because it fluctuated between 115 % DO and 155 % DO. Pure oxygen caused a significantly higher change in DO, which meant that a gentler control strategy had to be found. Therefore, a new controller was designed for the DO120 run , which is shown in figure 3.2. This shows the least variation relative to the set-point compared to the DO80 and DO30 run and also shows no spikes. This suggests that an interval control is more suitable than a pure PI control for controlling the DO via the diffusion tube. However, this statement is probably limited to the gassing system used. The PI controllers were based on PI control to increase the proportion of air or O_2 up to 1 L min^{-1}. Mixing of gases in the diffusion tube was poor, since the air/O_2 controller did not let enough air/O_2 through until a set value of 0.8 L min^{-1} was reached, so that a change in DO occurred. This could be due to the two different MFCs. Because of this behavior, the use of a PI controller was difficult, since the PI controller did not regulate for a long time and then set the air/O_2 MFC to maximum output. A comparison with controllers from other works is difficult, since a comparison with controllers from the field of fermentation is not considered meaningful and refolding works that deal with the DO are rarely found. In the work of Meneses-Acosta [53], the influence of the DO is considered and controlled, but in this work gassing was done via bubbles and the control of the DO was time delayed. Therefore, a comparison has been classified as not useful.[53]

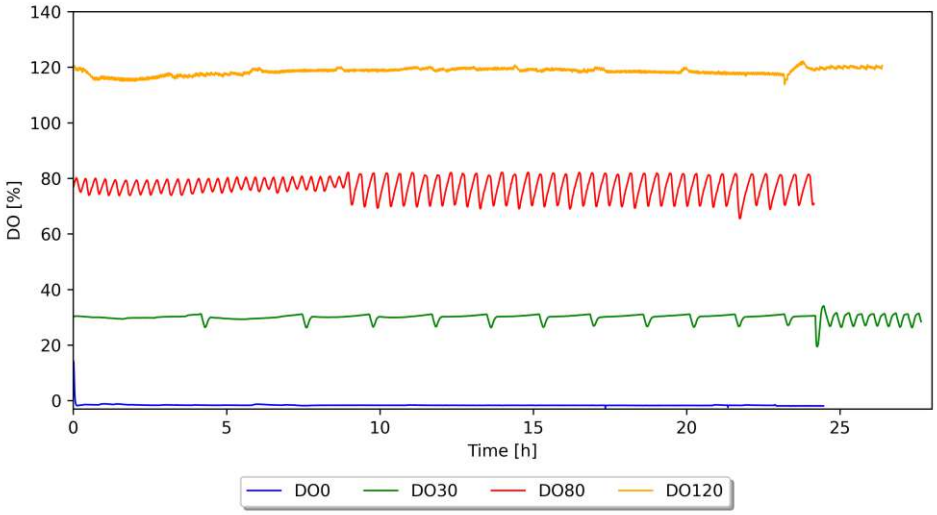

Figure 3.2: The measured DO concentration over time from the reactor runs where controlled to a constant DO.

During the runs at constant DO, the redox potential was measured inline, these measurement data are shown in figure 3.3. In all runs it can be seen that with the addition of the solubilisate the redox potential decreased by several 100 mV, which was probably due to the reducing agent TCEP. The jumps at the end of the runs were due to the addition of copper in the reactor. At the DO0 run, the lowest redox potential was observed. Furthermore, the redox potential increased over time for the DO30, DO80 and DO120 runs, but not for the DO0 run. For DO0 run, the redox potential decreased after the addition of solubilisate and after about 3 h it remained about constant. In the figure 3.3 it can also be seen that the higher the DO value was, the higher the redox potential was. These observations are consistent with the results of the work of Meneses-Acosta, who performed similar reactor experiments with alkaline phosphatase and chicken lysozyme.[53] The higher redox potential at higher DO is probably simply due to the fact that oxygen is a strong oxidizing agent. This influence of oxygen was therefore used for the runs at constant redox potential.

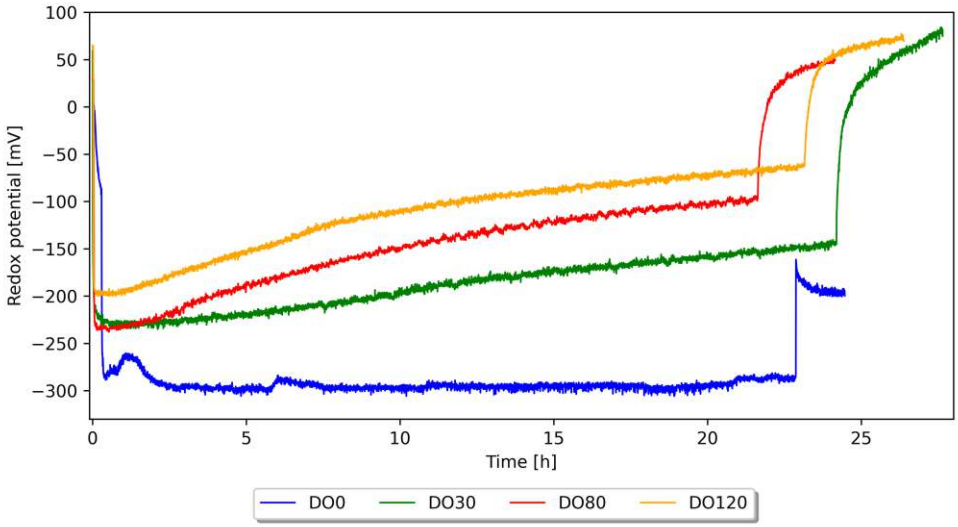

Figure 3.3: The measured redox signal over time from the reactor runs where controlled to a constant DO.

3.2.2 Redox controlled reactor runs

As already mentioned, in the reactor runs at constant DO, it was observed that the redox potential took on a higher value with increasing DO. Therefore, oxygen was used for the runs with constant redox potential. The additional generation of reactor runs at constant redox potential should be helpful in describing the influence of redox potential and DO on the refolding process of GalOx. The implementation of these runs was done in the same way as for the DO runs, that were via headspace gassing and the diffusion tube. Table 2.3 shows the runs with constant redox potential. In this table, the controlled parameter is also given for the respective run name. The Redox-300 run is the DO0 run, since this was approximately constant at -300 mV it was also used for the constant redox runs.

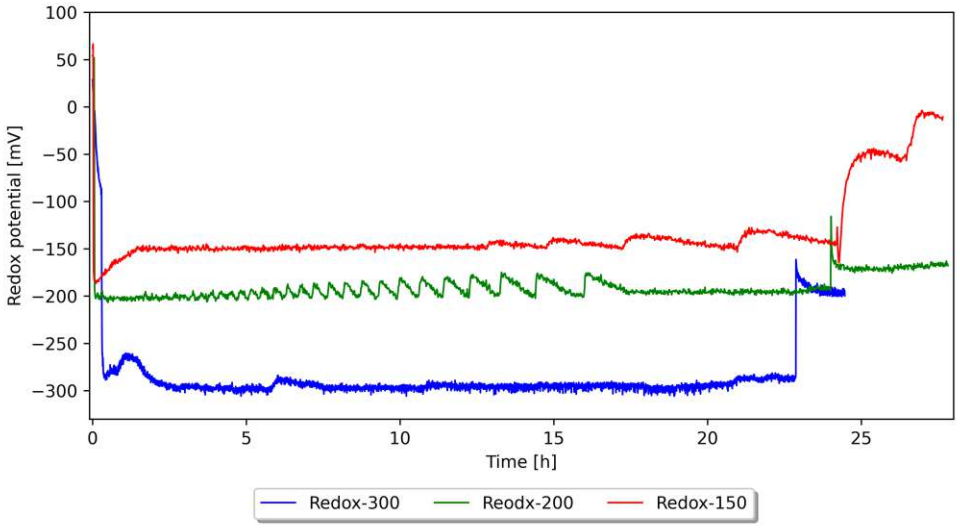

Figure 3.4: The measured redox signal over time from the reactor runs where a constant redox potential was controlled.

As with the DO runs, there was a drop in the redox potential after the addition of the solubilisate, which was probably due to the TCEP. At the end of the runs, a second change in the redox potential can be seen, which is due to the addition of copper. This jump was at about 23 h for the DO0 run and at about 24 h for the Redox-200 and Redox-150 run. In the case of the Redox-150 run, a jump in the redox potential could also be seen at 26 h, which could be attributed to the addition of oxygen (see figure 3.5). The addition of oxygen was due to a human error during sampling. Looking at the redox signal at the Redox-200 run it can be seen that short spikes in positive direction can be seen, these are from added oxygen. Attenuated variations of this can also be seen in the Redox-150 run. Looking at the DO curve of the redox runs in figure 3.5 and the measured cysteamine in form of TCEP equivalence concentration

from point 2.10.1, it can be seen that the higher the TCEP equivalence concentration was, the more oxygen was needed to move the redox potential in a positive direction. This was also the reason why the controller from the Redox-150 run was operating at 2 L min^{-1} to introduce as much oxygen as possible into the reactor. However, despite this measure and a DO value above 250 %, it took about 1.5 h until the set point of -150 mV was reached. Therefore, no more positive run was performed, since controlling the redox potential with oxygen would mean too long a setting time for such a set point. Furthermore, it should be mentioned that the spikes in the Redox-200 and Redox-150 run can be avoided by better regulating the oxygen content of the supplied gas depending on the TCEP equivalence concentration. In the figure 3.5 it can also be seen in the Redox-150 run that the measured DO was constant at 250 % for the first 4 h. This was due to the upper measurement limit of the DO probe, therefore no exact value could be given in this period. It can be assumed that the true DO value in this period was greater than or equal to DO 250 %.

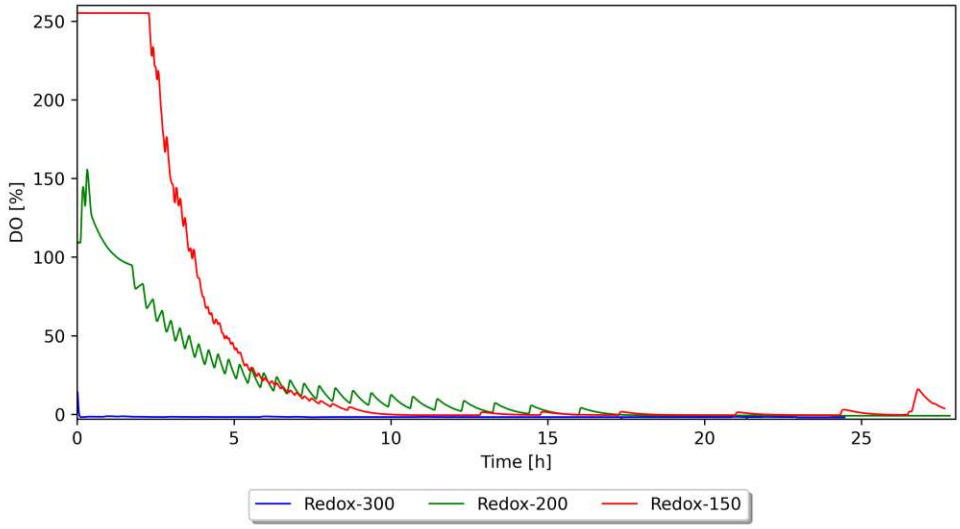

Figure 3.5: The measured oxygen over time from the reactor runs where the redox potential was controlled to a constant value.

3.3 Exploring the impact of DO and redox potential on activity

3.3.1 Impact on volumetric activity

In order to find out whether the DO is a CPP, it must be examined more closely. Consequently, the influence of the DO on the volumetric activity was analyzed. The volumetric activity as a function of time is shown in figure 3.6 for the different DO runs. All reactor runs started at a volumetric activity of about 0.13 U mL^{-1}. In the first 12 h of refolding, only the DO0 run showed an increase in volumetric activity. The DO30, run appears constant within the first 12 h. Possibly a weak tendency to a decrease in volumetric activity can be observed for the DO80 and DO120 run. Looking at the measuring points after 18 h, a similar behavior as after 12 h can be observed. The DO80 and DO120 run have decreased in activity compared to the initial value. The volumetric activity of the DO30 run showed no clear change over time. Only the DO0 run shows a higher activity compared to the start value. There was no clear difference between the activity measurements where the copper incubation took place in the reactor and externally.

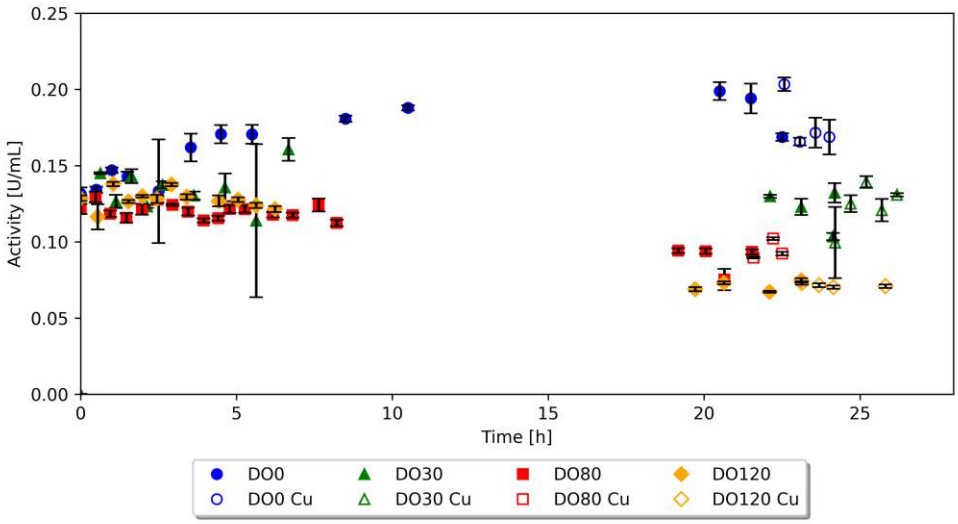

Figure 3.6: Course of the volumetric activity determined with the ABTS assay over time, of the reactor runs in which a constant DO was controlled. The data points with filling represent samples for which the copper incubation took place externally outside the reactor and the data points without filling represent samples for which the copper incubation took place in the reactor.

The runs from figure 3.6, give the impression that the enzymatic activity decreases with increasing DO. It is conceivable that, due to the high DO level, there is a reac-

tion between the oxygen and the protein or another component in the reactor. The amino acids cysteamine and methionine are among the most easily oxidized amino acids due to their sulfur group. The oxidation of such a group can affect the chemical and physical properties, leading to changes in confirmation, structure, solubility, stability and enzymatic activity.[92] Possibly, such oxidation could lead to the GalOx not being folded into its native form, which could be indicated by a decrease in activity. Furthermore, oxidation could also lead to the formation of more soluble aggregates with reduced or no activity. Possible oxidation reactions could be with the already folded protein as well as with intermediate protein. The reaction with native protein is necessary, however, because a decrease in volumetric activity was observed. In the case of already folded protein, oxidation in the active site could be problematic for its activity. The oxygen does not necessarily have to react with the protein, due to the oxidation of another component in the reactor, this could also be related, see point 3.3.4. Whether the refolding resulted in oxidation of a component in the reactor cannot be determined with the available data. Furthermore, the change in activity rate does not have to be directly related to the oxidation of the protein or a functioning substance in the reactor, since the oxygen also influences the redox potential.

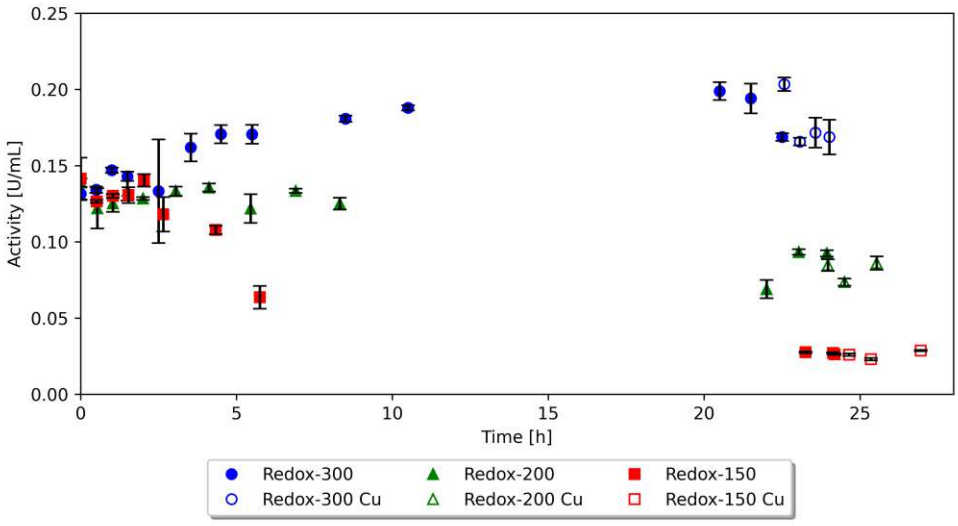

Figure 3.7: Course of the volumetric activity determined with the ABTS assay over time, of the reactor runs in which a constant redox potential was controlled. The data points with filling represent samples for which the copper incubation took place externally outside the reactor and the data points without filling represent samples for which the copper incubation took place in the reactor.

Looking at the reactor runs at constant redox potential, it can be seen that only the Redox-300 run, which took place under exclusion of oxygen, shows an increase in activity over severel hours. The Redox-200 run shows a constant to minimally decreasing volumetric activity in the first 12 h. The volumetric activity of the Redox-200 run shows a lower value after 18 h. For the Redox-150 run, a decrease in volumetric activity can already be seen in the first 12 h and was only a fragment of the initial value after 18 h. This induces the impression that a higher redox potential has a negative effect on the refolding or on the volumetric activity. There are several possible effects of the redox potential on the molecular level. It is conceivable that due to the higher redox potential there was increased oxidation in the reactor, which leads, for example, to oxidation of the protein. The higher redox potential could also affect refolding, as well as the proper formation of disulfide bonds. For example, the higher redox potential could increase the formation of disulfide bonds, which could result in more disulfide bonds being formed incorrectly due to the faster formation. In the case of the reactors runs at constant redox potential, the redox potential was controlled by oxygen. Considering the reactor runs at constant DO and constant redox potential, the question arises whether the decrease in activity can be linked to the DO and/or to the redox potential. By such a linkage a PAT tool for the industry could be developed. From an industrial point of view, a refolding of the GalOx should be done oxygen free or at a low redox potential to get maximum activity. The runs also indicate that for all reactoruns, refolding could probably be terminated after 5 min, since no significant increase in activity was observed after 5 min. With the exception of the DO0/Redox-300 run, this showed an increase in activity up to approximately 12 h. The comparison of these refolding runs with the literature is difficult, since on the one hand refolding data of GalOx are hardly available and refolding experiments are not actually carried out over such a long period of time. Furthermore, a comparison with proteins without disulfide bonds would be very difficult, because the information is very thin. In general, however, it can be assumed that the activity increases most strongly at the beginning of refolding and that the increase decreases over time.[12] This initial behavior can also be observed in the reactor runs and depending on the conditions the activity increases or decreases. In the work of Meneses-Acosta [53], in refolding experiments with alkaline phosphatase, the redox potential or the DO was also kept constant. In this work, however, the parameters were kept constant for only a few hours. No clear decrease in volumetric activity was observed in the DO runs of Meneses-Acosta [53]. However, in the runs at constant redox potential, a decrease was observed, as in the reactor runs at constant redox potential from this work.[53]

3.3.2 Protein levels and specific activity

The protein concentration in the reactors is interesting for several reasons. On the one hand, the protein concentration is a critical parameter in refolding and should therefore be monitored. Furthermore, it can be used to evaluate the developed bubble free gassing. The protein concentration is also an important parameter to explain differences in specific activity. It has been reported in the literature that gas/water interfaces such as bubbles or foam can promote the formation of protein aggregates [21, 87] and thus could also negatively affect the activity. This problem has already been described in point 1.5. For this reason, a bubble free gassing method was used to prevent the formation of protein aggregates. In order to assess the formation of insoluble protein aggregates, the protein concentrations of all reactor runs were investigated. Assuming that insoluble protein aggregates would be separated during the centrifugation step prior to protein determination, the formation of insoluble protein aggregates should lead to a decrease in protein concentration.

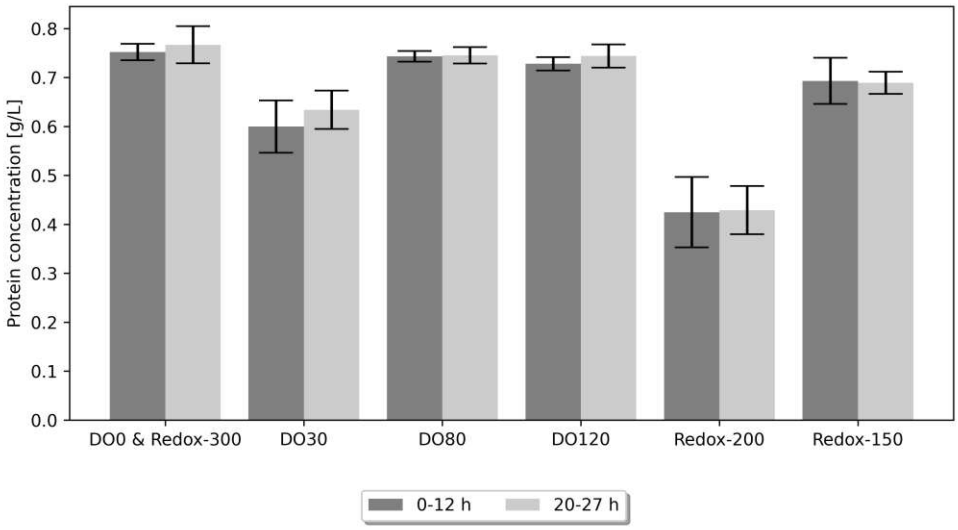

Figure 3.8: Bar chart of the average protein concentration of the reactor runs, additionally divided into two groups. One group results from the protein measurements from 0-12 h of a reactor run and the other group from the measurements from 20-27 h of a reactor run.

If the protein concentration is plotted as a function of time for each reactor, then no trend in protein concentration could be seen. Comparing the first sample of each run with the last sample of each run would be difficult, since single measurements are compared with each other. The reactor runs were performed over two days and no protein determination was performed at night. Therefore, the data points can be divided into two groups: protein determinations from 0-12 h and from 20-27 h. The

protein determinations between the groups are separated by at least 8 h, whereby the time separation was more for most reactor runs. The resulting values are shown in figure 3.8. In this figure , no noticeable differences can be seen between the protein determinations of the 0-12 h group and the 20-27 h group. Furthermore, it can be seen that the standard deviations always overlap with the mean value of the comparison value. In addition to the graphical evaluation, the mean values were compared with a t-test or Welch test. For this purpose, a Levene test for variance homogeneity was first performed. If variance homogeneity was present, a t-test was used. If there was no variance homogeneity, a Welch test was used. The calculated p-values are shown in a table in the appendix (Table 5.2). Assuming a significance level of 0.05 (same significance level for Levene test), it can be stated that no significant differences in the mean values between the 0-12 h group and the 20-27 h group are detectable. These observations allow the conclusion that the bubble free gassing method used either did not cause any or at least no measurable insoluble protein aggregate formation during the period tested. Therefore, assuming that the boundary conditions met are correct, the use of the developed bubble free gassing could prevent the formation of insoluble aggregates and prevent loss of protein concentration via the formation of foam. However, it is not possible to make a statement about soluble aggregates with the measurement method used. Comparing the protein concentrations between the reactor runs (based on the mean value the 0-12 h group and the 20-27 h group), no trend can be seen for the runs at constant DO. This is also the case for the runs at constant redox potential. Furthermore, it can be seen in figure 3.8 that the protein concentration of the runs at DO0/Redox-300, DO80, and DO120 were very similar, all of which were approximately 0.75 g L^{-1}. The Redox-150 run with 0.69 g L^{-1} was close to the DO0/Redox-300, DO80, and DO120 runs. The protein concentration of the DO30 with 0.62 g L^{-1} and the Redox-200 run with 0.43 g L^{-1} were relatively different from the other reactor runs. For these two reactors, it is possible that there was a problem with the solubilization, which could explain the difference. These different protein levels should be taken into account when looking for correlations, as this could have an effect on the activity.

Specific activity is a parameter that relates activity to protein concentration. Since the protein concentration in the refolding is a critical parameter, it should be observed. This was determined from the activity determinations with the ABTS assay and the protein determination by HPLC. The specific activity courses for the reactor runs with constant DO are shown in part A of figure 3.9 and the specific activity for the reactor runs with constant redox potential are shown in part B. As already mentioned in this point, the DO30 run and the Redox-200 run show a relatively different protein concentration, which was also visible in the specific activity. Both runs show a higher specific activity in relation to the other runs. The specific activity courses are similar to the volumetric activity courses. However, the runs appear more scattered, which can be attributed to the protein determination. Therefore, a multiple determination of the protein concentration would be recommended for future experiments.

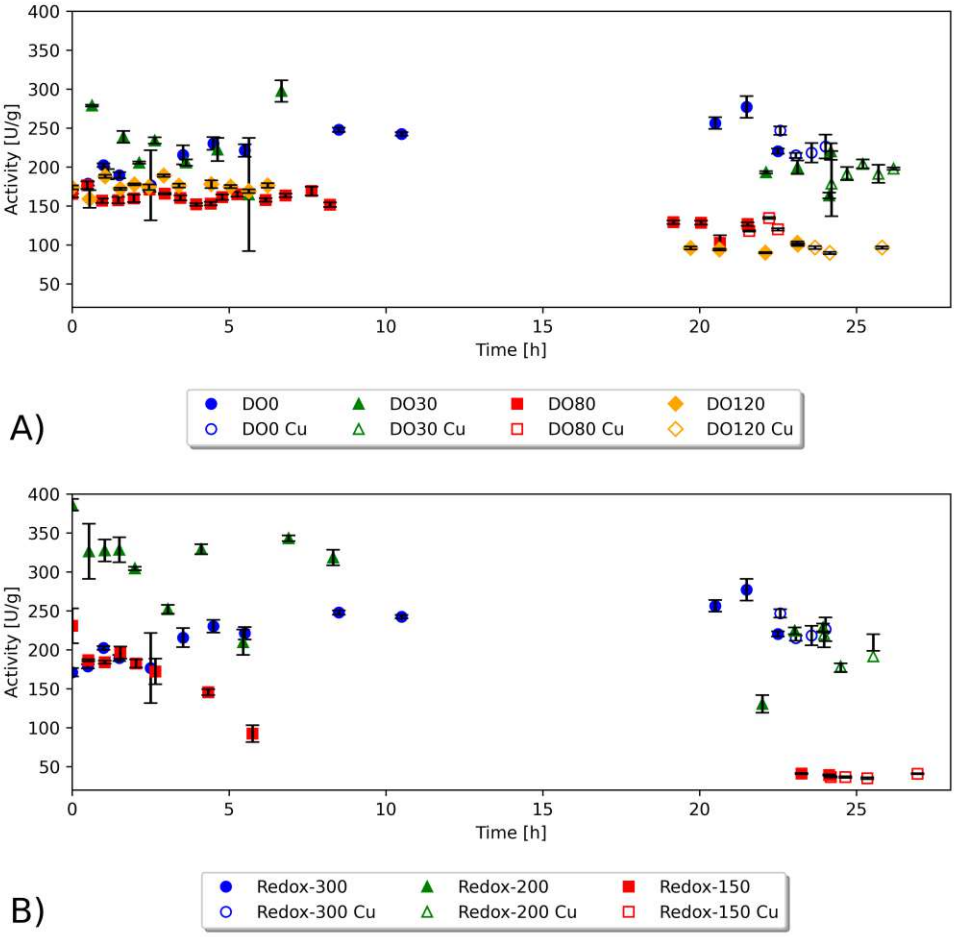

Figure 3.9: Course of the measured specific activity in the reactor runs. In part A the runs at constant DO are shown and in part B the runs at constant redox potential. In the case of the filled measuring points, the incubation with copper took place outside the reactor and in the case of the unfilled measuring points, the copper incubation took place in the reactor.

3.3.3 Concentration of free thiols

In Chapter 1.9, the basic behavior of the Ellman's assay has already been explained. The Ellman's reagent DTNB reacts with both sulfhydryl groups and TCEP, which complicates the interpretation of the Ellman's test results shown in Figure 3.10.

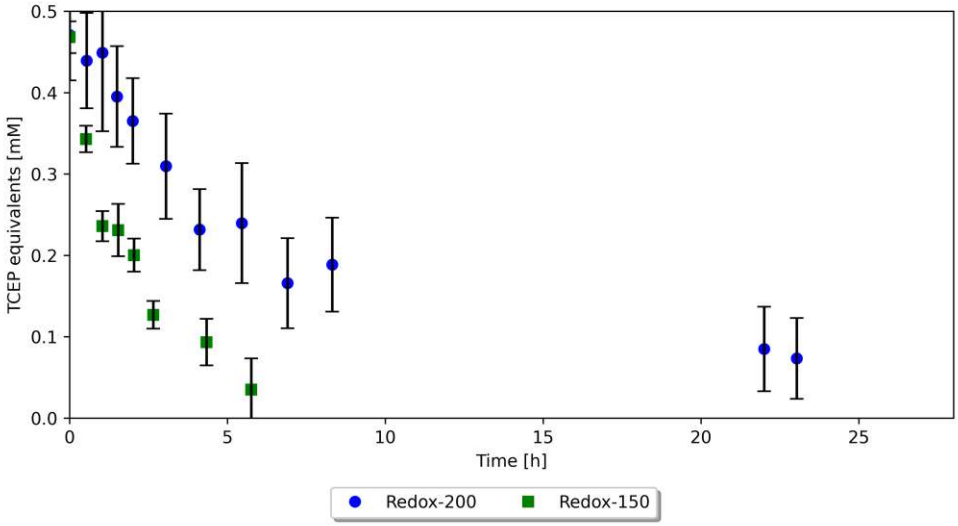

Figure 3.10: Ellman's assay measurement results as a function of time, from the reactor runs Redox-200 and Redox-150. The measurement results are shown in the form of TCEP equivalents.

Samples analyzed by the Ellman's assay were from refolding reactor runs in which several potential reactants for DTNB were present. The solubilization of the IBs used TCEP, which reacts with DTNB as mentioned earlier. This TCEP also reduces the cysteine bonds, which then consequently causes the cysteines to then have sulfhydryl groups, which also react with DTNB. [38, 56] Since TCEP not only reduces cysteine bonds, but also reduces disulfides in general, it can be assumed that it also reacts with cystamine, resulting in the formation of cysteamine, which also has a sulfhydryl group and consequently also reacts with DTNB.[19, 38] In summary, three potential reactants can be identified for DTNB in the measured samples. As mentioned in the point 3.3.2, the highest average protein concentration in the reactor runs was about 0.75 g L^{-1} . Assuming that this 0.75 g L^{-1} represents pure GalOx, a molecular weight of 72.823 kDa [34] results in a concentration of 0.01 mM for GalOx. According to the literature, GalOx has 7 [34] cysteine, so 0.07 mM of free sulfhydryl groups were present in the samples. In the point 1.9, the reaction equation was given with respect to DTNB, and to convert this to TCEP equivalents, the value must be halved (TCEP converts DTNB to two TNB), resulting in 0.035 mM TCEP equivalents for the protein. Based on this consideration, at most a concentration of 0.035 mM TCEP

equivalents could be explained by the protein. Consequently, the remaining measured signal would have to come from the added TCEP or the cysteamine arising from the TCEP. It is reported that TCEP almost completely converts cystamine within 30 min to cysteamine.[19] Based on these considerations, it is assumed that, at the latest from the second sample onwards, the measurement signal originated mainly from cysteamine. Therefore, the Ellman's assay can be used as a method to monitor the cysteamine concentration, which is essential for the oxido-shuffling system. However, this method has a limited accuracy due to the protein and due to the reaction rate of cystamine to cysteamine. Figure 3.10 illustrates the measured data of the Ellman's assay from the Redox-200 and Redox-150 runs. In all other reactor runs mentioned so far, the Ellman's assay was not used. Figure 3.10 plots the readings from the Ellman's assay as TCEP equivalents versus time. This representation was chosen because the concentrations were determined using a TCEP calibration curve and, as previously mentioned, the measurement signal cannot be assigned exclusively to one reactant. Converting the amount of TCEP added to the concentration in the reactor gives a TCEP equivalent concentration of 0.59 mM TCEP. For both reactor runs, the first reading was approximately 0.47 mM TCEP equivalents. This discrepancy could be due to the fact that, as mentioned in point 1.3, the IBs is not only composed of the recombinant protein but also contains cell components. It is possible that these cellular components reacted with TCEP and therefore could not be detected by the Ellman's assay. Another possible reason could be that TCEP is not stable in phosphate buffers. For example, literature reports that TCEP completely degrades within 72 h at concentrations of 350 mM.[38] However, this factor should have played rather a minor role. After the first measurement time point, the Redox-150 run and the Redox-200 run show different courses. The reason for the different courses was probably the different DO during the runs, because as already described in point 1.5, sulfhydryl groups can react with oxygen. It is possible that the cysteamine reacts either with another cysteamine or with a cysteine from the protein via an oxygen-mediated oxidation. If the cysteamine reacts with another cysteamine, cystamine is probably formed. This would only change the cysteamine and cystamine concentration, leading to a decrease in oxido-shuffling, which in turn has an effect on disulfide bond formation. If the cysteamine would react with a cysteine from the protein, this would lead to a post-translational modification and if this cysteine forms a disulfide bond in the native protein, this formation would probably not be possible with the modification, which are probably necessary for stability and function. However, if a second cysteine comes close in space, then probably via the oxido-shuffling system a dissulfide bond would then be formed in the protein after all. In summary, it would be thinkable that a higher DO leads to a faster degradation of the cysteamine, which supports the formation of disulfide bonds. If this is degraded faster, then this could lead to less effective disulfide bond formation. If this logic is applied to reactor runs at constant DO or constant redox potential, then the increase in activity over time should be lower for runs with higher oxygen levels than for runs with lower oxygen levels. This behavior was also observed, but a decrease in activity was also observed in the reactor runs, which could possibly be due to an oxidation of the protein.

3.3.4 Investigation of correlations

In point 3.3.1 the first impression of the influence of the DO and the redox potential was already mentioned. It could be observed in the reactor runs that with a higher DO as well as a higher redox potential the activity decreased over time. It should be mentioned that the DO has a positive influence on the redox potential, which complicates the interpretation of the reactor runs. Furthermore, as described in chapter 3.2.1, the redox potential was regulated by the DO during the redox runs. To better understand the influence of these two parameters, they were considered in more detail. In a first step, pairplots of all collected data were created. The reciprocal value, the quadratic form and the logarithmic variant of the parameters and the activities were also included. As an example, a pairplot of the activities against the redox potential and against the DO is shown in figure 3.11. Since the measured values for protein determination were scattered and no trend was discernible in them, the mean values of the protein concentration of a run were used for the pairplots to determine the specific activity.

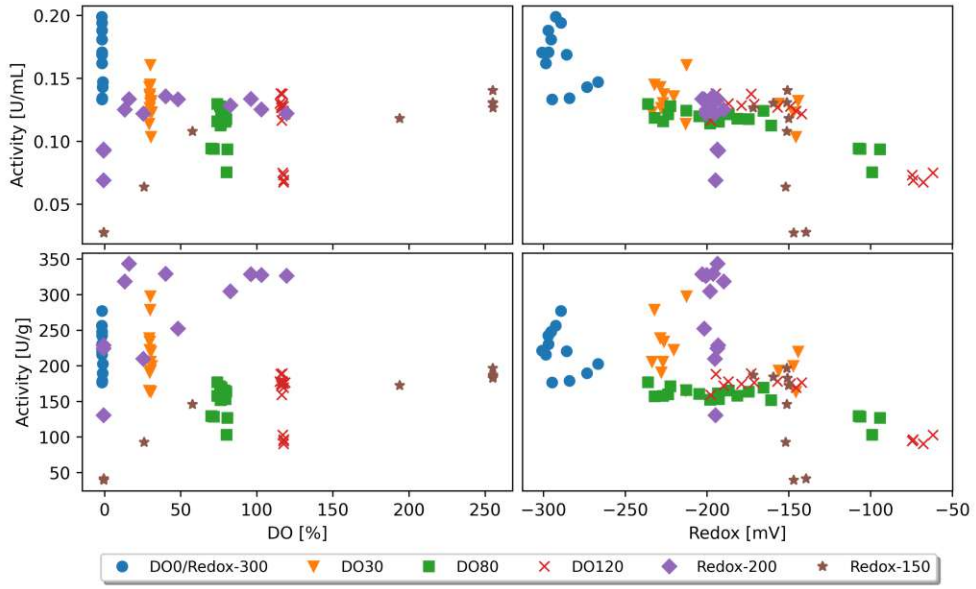

Figure 3.11: The figure, which consists of four individual graphs, shows the volumetric activity and the specific activity versus the DO, and against the redox potential of the reactor runs performed. The top two graphs refer to volumetric activity and the bottom two to specific activity.

Plotting the DO against the volumetric activity, no obvious linear relationship was apparent. The runs at constant DO behaved as vertical straight lines, corresponding to the DO kept constant. The DO0/Redox-300 run performed similarly. The Redox-200

and the Redox-150 run behaved differently, these show a horizontal course in the plot without a clear connection. The same behavior can be seen with the plot DO against the specific activity. Furthermore, a t-test was used to check for linear regression and no significance was found for the regression parameter ($\alpha = 0.05$). Consequently, neither visually nor via a statistical test could a clear correlation be established here. In the plot volumetric activity versus redox potential, the runs also behave as vertical straight lines at constant redox potential, which was expected according to the redox potential kept constant. The DO runs showed a horizontal distribution with a slope. Looking at the pair plot with the volumetric activity versus the redox potential gave the impression that a linear function could be put through the data points. If this was done and then tested for significant using a t test, the regression parameter was also indicated as significant by the t test ($\alpha = 0.05$). However, this has to be considered with high caution. A condition for linear regressions is no autocorrelation, however a positive autocorrelation can be determined over the Durbin Watson test [27] and from the logic of the data one is present. Furthermore, the regression would also only show an R^2 of 0.548. Looking at the specific activity against the redox potential, one gst a weaker impression of the linear relationship (between activity and redox potential), on the one hand because of the higher resolution of the data due to the y-axis, on the other hand also the position of the measuring point cluster changes from constant redox runs. Since the specific activity also has takes into account the critical parameter protein concentration and in this less a linear relationship was recognizable, the linear course of the volumetric activity should be considered critically. In reactor runs at constant DO, there was an increase in the redox potential and a decrease in activity over time with the exception of the DO0/Redox-300 run, so the linear trend could also be due to a decrease in activity over time. Since more DO runs than redox runs were performed, this reinforces the impression that a linear relationship is present in the redox versus volumetric activity plot. In summary, the pairplots do not show a clear correlation, but a possible connection between volumetric activity and redox potential, which should be considered very critically. There may be several reasons why no clear correlation could be identified. One could be that these two signals only had an indirect influence. The possible connection between the redox potential and the volumetric activity could indicate this. Another possibility could be that the complexity of the system was too high to be able to detect a clear correlation with simple approaches. However, a systematic error could also explain the lack of correlation. For the pairplots, only the redox value or the DO value that prevailed at the time of sampling was used; consequently, the course between the samplings was neglected, just like the time. To circumvent this possible problem, an attempt was made to create a kind of white-box model using known protein kinetics, in which the value of the redox potential as well as the DO is continuously included. The on-pathway model of Dill and Chan was used for this purpose .(see point 1.10) However, solubilization was neglected because no data were available from them. Consequently, the basic protein kinetics model consisted of intermediate protein and native protein, which can react reversibly. (See item 2.11) First, manually attempted to find a good fit over the protein kinetics model used by introducing a wide variety of DO and redox potential variants into the rate constants k_{ni} and k_{in}. However, manually could not find a fit that was considered

acceptable. In the manually attempts, several observations were also included one rate constant. This was not done in the systematic approach because the resulting models were considered too high. Therefore, as described in point 2.11, a systematic approach was followed, in which a large number of simple models were parameterized on the existing data. In sum, 6 times 930 models were tested on the data. The reactor runs used for parameterization are listed in table 2.7. The DO80 and the Redox-200 had different protein concentrations compared to the other four reactors runs and the exact influence of these is not known, therefore these were not used for the parametrization. (see point 3.3.2) Furthermore it was to be mentioned that the Redox-150 run of the DO0/Redox-300, DO80, and DO120 deviates proportionally most strongly, however with this a boundary condition was driven (highest DO value), therefore this was nevertheless used for the parametrization. Another problem with the Redox-150 run was that the DO value was above the detection limit of the probe for the first few hours of the run and therefore no accurate data was available. In figure 3.12, point A shows the RMSE of the best model of the corresponding model variants. In this part A it can be seen that despite this number of models, no model could be found that had an RMSE below 80. The model with the lowest RMSE is a model using a first order degradation reaction from the native protein.

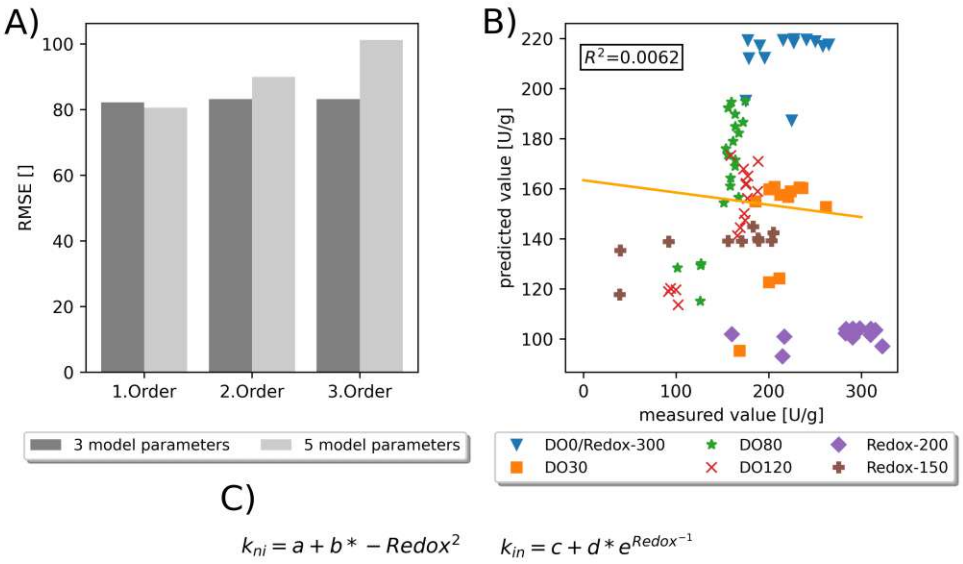

Figure 3.12: Results from the attempt to establish a mathematical relationship between the activity and the redox potential and/or the DO. Part A contains the RMSE of the best model found using the permutation approach corresponding to a first, second or third-order back reaction. Part B includes measured vs predicted plot of the model with a first order backreaction. Part C contains the formula of the best model with 5 model parameters and a first order backreaction.

Part C of this figure shows the composition of this model and part B plots the simulated values against the measured values. It can be seen from part B that agreement of the values was limited. Looking at the RMSE values of the best models in more detail, it can be noticed that at second and third-order the best models with three model parameters show a lower RMSE than those with 5 parameters. It should be mentioned here that, as described in point 2.11, all parameters were parameterized together after the screening . Consequently, in the models with 5 model parameters, 5 model parameters were parameterized at the same time, which may have led to a problem.
In summary, also with the systematic approach using white box models structure, no correlation could be found. Reasons for this could be, as mentioned before, that the tested parameters only have an indirect influence, that complex dependencies exist, or that a systematic measurement error prevails. Another possibility to examine the data would be for example a partial least square (PLS) model, but this is based on linear regressions and since no clear correlations could be found in the pairplots, it is assumed that this would also have only a limited power. [86] Also possible would be the use of a black box model, like a neural network. However, it is assumed that there is not enough data to set up and train such a system.[1] A PLS model as well as a neuronal network would not show how the DO as well as the redox potential affect the refolding process and were therefore not classified as useful and therefore not carried out. As already mentioned in this chapter, the DO or the redox potential could have predominantly only an indirect influence on the refolding process. An interesting parameter that may play an important role could be the cysteamine concentration, which has already been described in point 2.10.1. Cysteamine is essential for the oxido-shuffling system and thus causes the formation of disulfide bonds.(see point 1.5) In figure 3.13, the cysteamine concentration in the form of TCEP equivalents is plotted against the activities. The cysteamine concentration was only measured in two reactors runs, the Redox-200 and the Redox-150 run. Looking at the volumetric activity versus the TCEP equivalents (cysteamine concentration) , similar courses can be seen, so this could be an interesting parameter. Since only two runs with such data were available and they differ only by 50 mV in the redox potential, it was decided not to create a model.

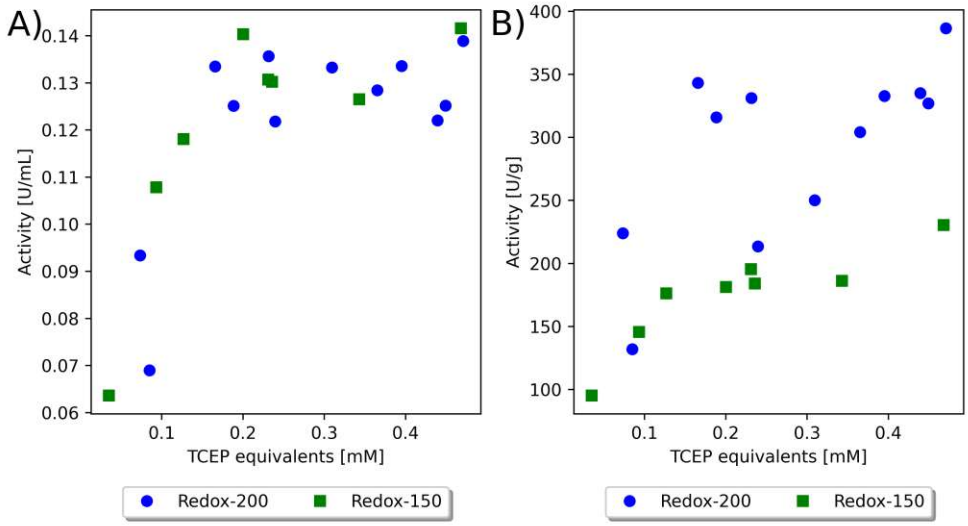

Figure 3.13: The figure shows the activity against the TCEP equivalences of the Redox-200 and Redox-150 reactor runs determined by Ellman's assays. Part A of the figure shows the volumetric activity and part B the specific activity.

In general, neither with the pairplot nor with the systematic approach a clear correlation could be observed. With TCEP there are at least similar courses in the pairplot. Probably the approach used was too simple for the system used. Several mechanisms could play a role in the used system. It is possible that the DO plays a role via an oxygen mediates system, the DO also causes a degradation of the cysteamine, which can have an influence on the activity via the redox shuffling system. Furthermore, it is also possible that high DO levels lead to oxidation of the protein. In the protein kinetics model used, only intermediate protein was present and native protein, therefore solubilised protein was neglected which may also be a problem as the amount of protein used was not taken into account. This model also neglects the formation of aggregates that can occur in the refolding process. [58] The protein concentration used also refers to the total protein concentration and not to the GalOx concentration. Furthermore, the measured protein concentration neglects insoluble aggregates, which are lost during the centrifugation step. In the end, the effect of DO and redox potential could not be described more precisely with the 6 runs performed. Under the assumption that the used system is too complex to describe effects by simple correlations, an alternative oxidant was searched for, in order to possibly allow a simplification.

3.4 Screening for alternative oxidation agents

3.4.1 Alternative oxidants

In the reactor runs where the DO and the redox potential were controlled separately, no clear correlations could be found, so an alternative oxidant was sought to replace oxygen in order to influence both parameters as independently as possible. For this purpose, classical oxidizing agents and oxidants from the literature were tested to see what influence they had on the volumetric activity. The tested substances which had an influence on the redox potential are listed in table 3.2. In addition, sodium chlorate and cystsamine were also tested. Sodium chlorate was added up to a concentration of 75 mM, but showed no effect on the redox potential. Dissolving the sodium chlorate was done in an ultrasonic bath, it was assumed that this caused the conversion to NaCl and therefore there was no effect. Cystamine, which is popular for oxido-shuffling, was also added up to a concentration of 6 mM, but caused no discernible change in redox potential. Another classic oxidant, which can also be found in the literature, is H_2O_2. This was not tested here as the ABTS assay used this for the color change. Table 3.2 shows that all the oxidants tested in the table influenced the redox potential, but at the same time also had a significant effect on the enzyme activity. The GalOx was presumably oxidized in this process. Interesting targets for the added oxidizing agents are methionine and cystamine, due to their sulphur group. However, oxidation of the protein backbone would be possible. [92] Further analytical methods such as mass spectrometry (MS) data would be required to make more accurate conclusions. The delta redox in Table 3.2 always refers to the change in redox potential before the first addition of an oxidant. It is assumed that the oxidants tested have interacted with the active protein. The reason for this assumption lies in the reactor runs with constant redox potentials, since similar redox potentials have been also measured in these reactor runs and they did not lead to such high decreases in activity (in a period of a few hours). Therefore, the oxidants listed in Table 3.2 were classified as not usable.

Table 3.2: Oxidising agents that caused a change in redox potential.

Oxidation agent name	Oxidation agent [mM]	Δ Activity [%]	Δ Redox [mV]
Iodine	0.42	63	40
	0.56	no activity	100
Potassium hexacyanoferrate(III)	0.13	98	20
Potassium tetrathionate	0.07	10	20
	0.71	94	150
Potassium permanganate	0.34	93	300

3.4.2 Effects of copper incubation

After no alternative oxidation agent was found, the idea of using copper to regulate the redox potential was considered. However, it must first be clarified whether the added copper concentration and the time of copper addition have an influence on the enzyme activity. Therefore, to determine whether copper was suitable for this purpose, a DoE was performed with respect to the copper concentration and the timing of copper addition. Of these DoEs, the contour plot is given in figure 3.14. For this DoE, only those therms were used whose influence was greater than the 95 % confidence interval. More detailed information on the DoE is given in the form of an overview diagram in the appendix. The model accuracy was considered sufficient for the determination of influence. For the model fit, it should be noted that all activities determined via ABTS were measured within 10 min, which led to the measurement accuracy. The Contour plot shows that the copper concentration and the time of copper addition have an effect on the specific activity. According to the model, the highest activity is expected at a low copper concentration and a late copper addition. Therefore, if copper is used for redox adjustment, it would be questionable whether the influence of the redox potential causes the activity change or the time or concentration of the copper addition.

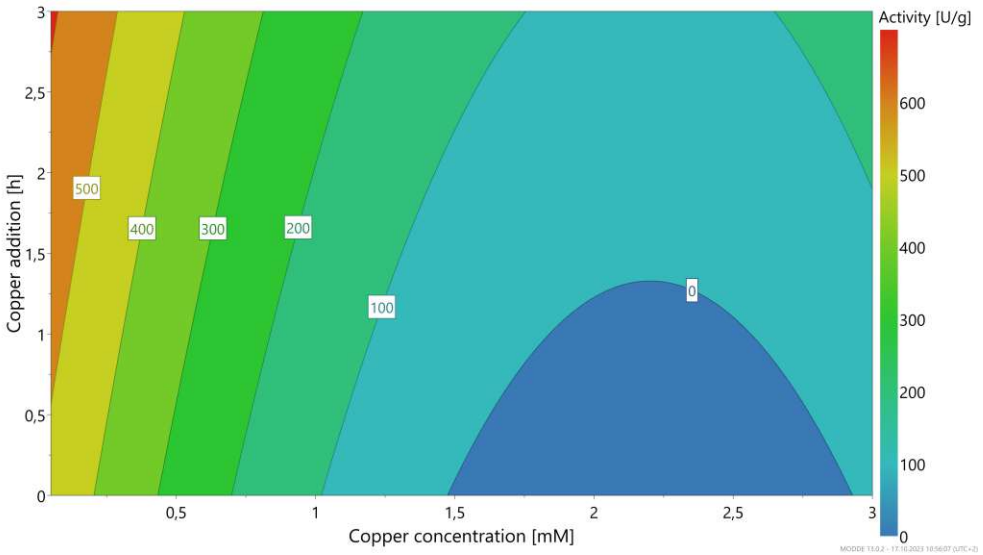

Figure 3.14: Contour plot of the DoE related to the copper concentration and time of copper addition. The time of copper addition in h is on the X-axis and the copper concentration in mM is on the Y-axis. The color highlighting represents the specific activity. For the MLR model, an R_2 of 0.882, a Q2 of 0.841, a model validity of 0.722 and a reproducibility of 0.878 were calculated.

3.4.3 Characterization 3MBA assay

After no alternative oxidant could be found, a way to make H_2O_2 usable was sought. H_2O_2 was found to be promising since GalOx catalyzes its formation. An alternative 3MBA assay was found in the literature, which also allows activity determination like the ABTS assay. Before using this assay, it was first examined in more detail, since according to the literature the assay is many times less sensitive than the ABTS assay. First, a wavelength scan was performed to get a more accurate overview. The highest absorbance change between the product (alcohol) and reactant (aldehydes) was determined at 312 nm. The wavelength scan is shown in part A of figure 3.15. Since the extinction coefficient of 314 nm was given in the literature and the absorbance difference between 314 and 312 nm was small, it was decided to use 314 nm for all further measurements. Part B of figure 3.15 shows absorbance scans at different 3MBA concentrations. This figure shows that the higher the 3MBA concentration, the higher the absorbance change over time. The highest absorbance change could be observed at a 3MBA concentration of 200 mM, but at this concentration two phases could be detected in the mastermix, so it was decided to do all further tests with a mastermix of 150 mM 3MBA, since at this concentration the highest absorbance change could be detected in homogeneous mastermix.

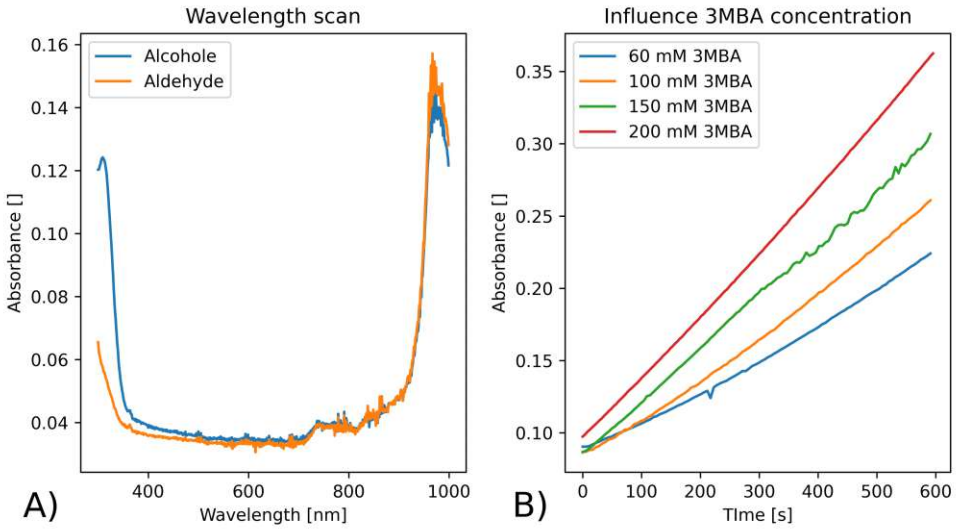

Figure 3.15: A) Wavelength scan of 3-methoxybenzyl alcohol before the addition of GalOx and 10 min after the addition of GalOx (3-methoxybenzyl aldehyde). B) Time-dependent absorption measurement of the 3MBA assay at different 3MBA concentrations of the mastermix.

Next, an optimal ratio between sample and master mix was sought. The absorbance scans from this can be seen in figure 3.16 in part A. The total volume chosen here was 300 µL. The highest slope could be detected at a ratio of 200 µL master mix and 100 µL sample. Once the absorbance wavelength, 3MBA concentration and sample to mastermix ratio were chosen, it was tested if the assay was H_2O_2 tolerant. An absorbance scan can be seen in figure 3.16 part B, in this test H_2O_2 was added to the sample and blank and it can be seen that there was activity and the blank remained unchanged. These features indicate that the 3MBA assay can be used for activity determination in the presence of H_2O_2.

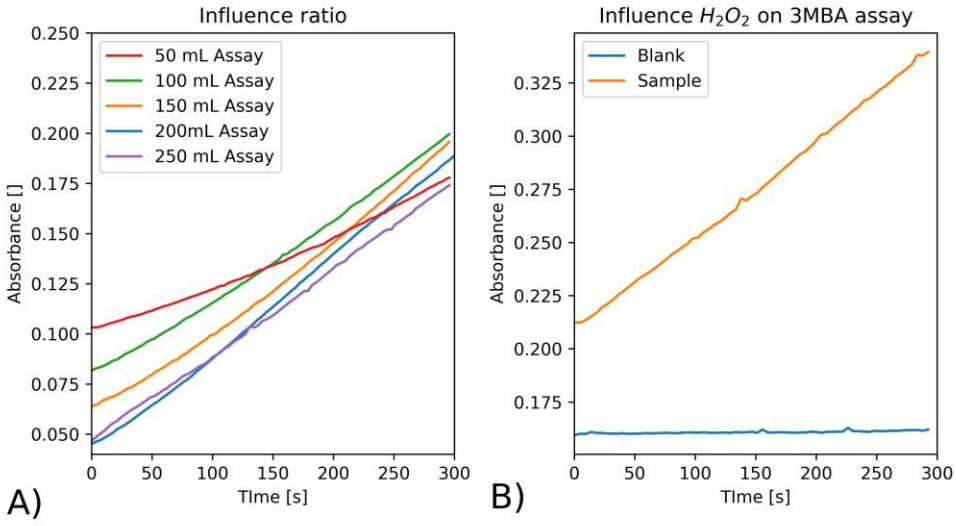

Figure 3.16: A) Time-dependent absorbance measurement of the 3MBA assay at different vorlum ratios between mastermix and sample B) Time-dependent absorbance measurement of the 3MBA assay with addition of H_2O_2 to the sample and the blank.

To establish comparability between the 3MBA assay and the ABTS assay, the activity was determined at different GalOx concentrations. The determination was performed with the ABTS assay and the 3MBA assay, the results of which can be seen in figure 3.17. The blue markers represent the course of the 3MBA activity determinations. This activity appears to increase linearly with increasing GalOx concentration, which is the expected value, based on the assumption that more active enzyme leads to a higher measured volumetric activity. The green dots represent the activity measurements of the ABTS assay, the course of which was unexpected. From 0.01 g L^{-1} to 0.25 g L^{-1}, the activity increased and then decreased despite the higher GalOx concentration. The course of the ABTS assay indicates that the linear progression of the assay was several times smaller compared to the 3MBA assay. The set concentration range did not allow

to determine a coefficient to match the 3MBA assay to the ABTS assay. However, this comparison revealed an interesting point that could explain the lack of correlations from the reactor runs.

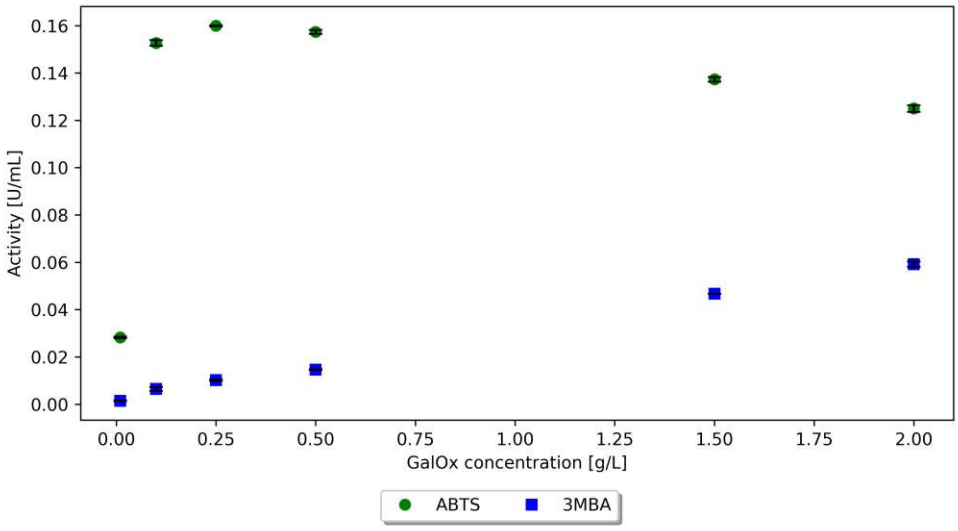

Figure 3.17: Enzyme activity measured by ABTS assay and 3MBA assay at different concentrations of GalOx (standard).

3.5 Limitation of detection and the approach used

In the comparative measurements of the ABTS assay and the 3MBA assay, it was observed that the linear range of the ABTS assay was possibly a problem for the reactor runs. It should be noted that in the reactor runs, all activity determinations were made undiluted, with the ABTS assay, as there was no sign of limitation of the assay. However, the observations made in the comparison runs (see figure 3.17) are not directly transferable to the reactor runs, since the amount of active GalOx was probably lower in the refolding samples. To determine whether the possible small linear range of the ABTS assay was a problem in the reactor runs, a refolding sample was diluted several times to determine whether the measurements could be in the linear range. The results from this are noted in figure 3.18. The data point with the highest concentration is an undiluted refolding sample, and the data points with lower concentrations are serial 1:2 dilutions. In this it can be seen that the undiluted sample was not in a linear correlation to the dilutions. This suggests that possibly the measurements of the reactor runs are falsified, since the measurements have been outside the linear range. This would be an explanation for the lack of correlation finding in the reactors.

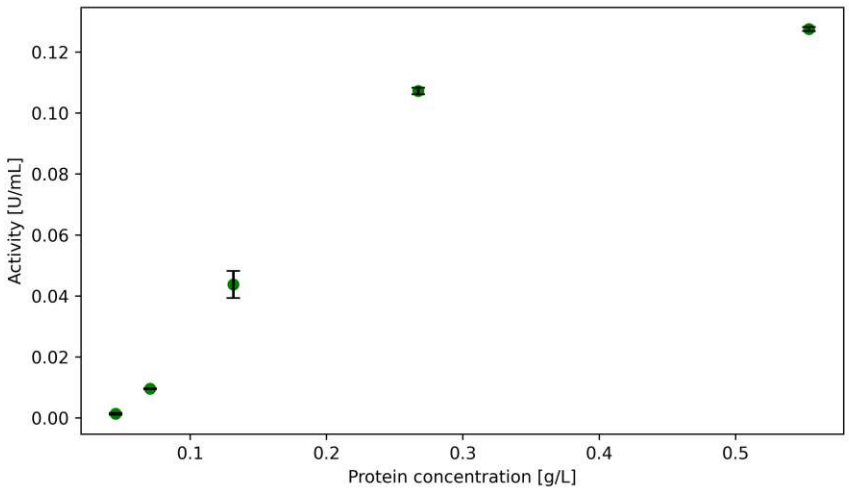

Figure 3.18: Activity determination of a refolding sample at different dilutions. The measuring point with the highest protein concentration represents the undiluted sample and the remaining measuring points are a sequence of 1:2 dilutions.

To better assess the linearity problem of the ABTS assay, a repeat reactor run was performed in which the volumetric activity of multiple dilutions were always measured. In order to allow comparability, a taget value from a previously performed run was chosen. Since the run at a DO concentration of 0 % have been used both for the comparison of the DO runs and for the comparison of the redox runs, and since this runs showed the highest volumetric activity of all the runs performed, it was decided to repeat this run with dilution measurements. For this purpose, dilutions of up to 1:8 were used. The determined activity is shown in figure 3.19 as "DO0 new". In this figure, the previously performed DO0 without dilutions is also indicated as "DO0". Regarding the protein concentration of the DO0 new, a mean protein concentration of 0.61 g L^{-1} could be determined, which was similar to the last DO0 run, which was at approximately 0.75 g L^{-1}. Comparing the two DO runs, it can be seen that activity measured via dilutions was higher. Furthermore, the run at the end appears slightly different, with the DO0 new the activity increased over night, with the old DO0 run the activity appeared about unchanged, possibly slightly increased. Also, the new DO0 run shows that on day two the activity was at a constant value and with the DO0 run the activity on the second day seems to be slightly decreasing or constant.

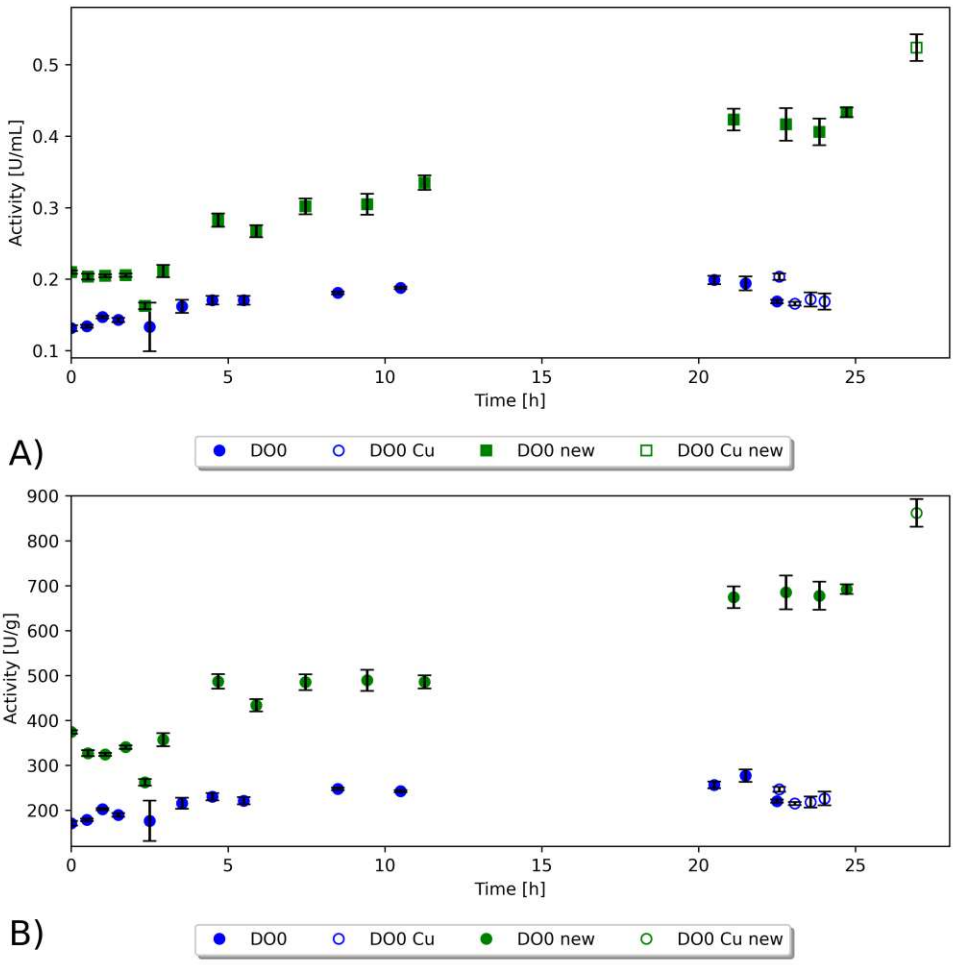

Figure 3.19: Comparison of the activity resulting from the ABTS assay with and without dilutions in a DO0 reactor run. DO0 represents the original run where no dilutions were measured. DO0 new represents another reactor run in which the activity determination was determined over multiple dilutions. The plotted activity represents the maximum measured activity of the measuring series. Part A shows the volumetric activity and part B the specific activity. For the data points with filling, the copper incubation took place outside the reactor and for the points without filling inside the reactor.

In summary based on the DO0 and DO0 new it is assumed that the small dynamic range of the ABTS assay can be classified as a problem. Other volumetric and specific activities could be measured over the dilutions. Possibly also a different course can

be interpreted. Looking at the behavior of the ABTS assay at different Galox concentrations in figure 3.17, it can be seen that the assay shows an increase in activity at low GalOx concentrations, then goes into a platou phase and then the activity decreases with increasing GalOx concentration. Based on this curve, it is not possible to estimate the influence of the small dynamic range on the other runs. Therefore, all reactor runs should be repeated, using multiple dilutions to determine the volumetric activity, in order to find dependencies.
In the attempt to mathematically describe the influence of the redox potential and the DO on the refolding process of GalOx, a too simple system was used in the method described here. In order to be able to describe the influence of these parameters, the interactions of the individual components/influencing variables must be better recorded and understood. In the runs at constant DO, as well as at constant redox potential, there was a decrease in activity compared to the initial values. This is described in point 3.3.1. Since oxygen has been used for regulation in these runs, this indicates that oxidation of the protein probably occurred. Therefore, the influence of oxygen on GalOx should also be investigated independently of refolding in order to be able to characterize this influencing variable independently. It may also be possible to use an alternative protein that is less sensitive to oxidation. Another connection that should be investigated are the interactions of the reducing agent TCEP, which were described in point 2.10.1. Based on the literature and the available data, it is assumed that this probably reacts with the phosphate buffer, the protein, the remaining IB components and the cystamine. The reaction of cystamine to cysteamine appears to be particularly interesting, since this presumed reaction leads to the formation of an oxido-shuffling system, which is supportive for the disulfide bond formation. However, this should be confirmed via, for example with MS measurement. The TCEP equivalent courses show a decrease over time, which is probably caused by the DO. Since these TCEP equivalents are probably cysteamine and this has an influence on the formation of the disulfide bonds, their reduction should be better characterized or considered individually. Another system that has an influence on the formation of disulfide bonds is the oxigen mediated system, which acts via oxygen. Consequently, the DO is involved in several mechanisms that could have an influence on refolding or enzymatic activity: oxidation protein, cysteamine concentration (oxido-shuffling), redox potential, oxigen mediated system and possibly soluble aggregate formation. In point 3.3.2 it was already mentioned that no difference in the protein concentration could be determined over time or that no difference was recognizable with the method used. Nevertheless, the protein determinations showed a certain scatter, which was clearly visible in the specific activity. Therefore, it would be advisable to measure multiple determinations of the individual samples, since the additional effort is low and a multiple determination allows a better statement about possible insoluble aggregates. Regarding the protein concentration, it would also be beneficial to determine the amount of GalOx in the IBs, as this can be considered as a main parameter. Furthermore, the protein concentration of the solubilisate should also be determined and included in the mathematical description. In addition, the presumed oxidation of the protein should also be considered as a term in a modeling, as well as the formation of aggregates. In this experiment, the formation of soluble aggregates was neglected, which may pose

a problem. Therefore, a measurement method should be used to avoid this problem. Conceivably it would be possible via an absorption measurement, size exclusion measurement or via light scattering measurement. As already mentioned in this point, there was a problem with the dynamic range of the measurement in the reactor runs when determining the volumetric activity. This problem was very problematic for the data presented in this thesis, but can be circumvented by diluting the activity determination. Alternatively, one could try to optimize the ABTS assay to generate a larger linear range. Probably due to the reasons given here, it was not possible to set up a model for the DO and the redox potential.

4 Conclusion

According to the knowledge gained from this work, the scientific questions can be answered as following:

- Can the DO be controlled in a refolding process, and if so, what is the technical implementation and control strategy?

The DO concentration in a refolding process could be controlled bubble free in several reactor runs. In this work, a combination of membrane gassing via a diffusion tube and headspace gassing was used. It should be mentioned that membrane gassing has a much higher $K_L a$ than headspace gassing. Through the additional use of the diffusion tube, the $K_L a$ could be increased by more than 600 %, compared to pure headspace gassing. Despite the combination of these two methods, the resulting $K_L a$ cannot be compared with that from gassing via bubbles, since it is much lower. In order to place the diffusion tube efficiently in the reactor, a holder had to be developed for it, which, due to the space limitations in the reactor, required a compromise between the stability of the holder, the effective diffusion area of the tube and the distance between the components in the reactor. PI controllers and interval based controllers were used for the reactor runs where the DO was kept constant. Both controller types basically allowed control of the DO. However, better control of the DO was observed using the interval based controller. The reason for this is probably due to the insufficient mixing of the gases from the different mass flow controllers.

- How can the redox potential be controlled in a refolding process using DO, what is such a control strategy and are there alternative oxidants to control the redox potential?

A controller based on the DO has been designed for reactor runs to maintain a steady redox potential. The principle of the controller is based on supplying air or O_2 below the target redox potential and N_2 above the target redox potential. It should be noted that the sensitivity of the redox potential increases with time, which is probably related to the measured TCEP equivalents (cysteamine concentration). Furthermore, it should be mentioned that the developed controller only allows a positive regulation of the redox potential. In the presented work, several oxidants were tested as an alternative to O_2. All tested alternative oxidants caused a massive reduction of the enzymatic activity. Compared to O_2 as an oxidant, the activity of the tested oxidants decreased several times more at a similar redox potential. The only oxidant that showed promising results was H_2O_2, but this is not compatible with the ABTS assay, which uses H_2O_2 to determine activity. Therefore, the ABTS can not be used in

processes utilizing H_2O_2 as oxidant. An alternative assay, the 3MBA assay, is suitable for those cases but is considerably less sensitive.

- How does the redox potential or the DO influence the activity of the GalOx during refolding?

In the runs at constant DO it could be observed that with higher DO the activity decreased more strongly over time. A similar behavior was observed for the reactor runs at constant redox potential. With these the activity decreased with higher redox potential. However, the regulation of the redox potential occurred via the DO. Consequently, on average a higher redox potential was caused by a higher DO. It is therefore difficult to determine whether the DO was the cause or the redox potential, or both, of the change in activity. It should also be noted that only in the reactor run with the lowest redox potential, which was oxygen-free, an almost continuous increase in activity was observed. In refolding, the expected activity increases over time, whereas the increase over time decreases. This behavior was only observed in the DO0/Redox-300 run, all other runs showed a decrease in activity over time.(compared to start value) However, the activity data must be considered carefully, since it can be assumed that not all measurements were made in the linear range of the ABTS assay.

- Is it possible to establish a mathematical link between the activity and the DO and/or the redox potential, that can then be used for a potential model?

The influence of the DO or the redox potential could not be described mathematically, therefore no suitable model could be set up. The DO was used for the regulation of the redox potential, therefore it was not possible to consider these two parameters independently. Furthermore, the data from this work suggest that DO is involved in a variety of mechanisms such as: Oxidation of the protein, reduction of the supposedly formed cysteamine (oxido-shuffling system), formation of disulfide bonds (oxidation mediated system) and the redox potential. In the approach of the work too many influencing variables were not sufficiently considered, whereby the construction of a model was not possible. Furthermore, problems regarding the linear range of the activity determination were identified, which made an accurate description of the system more difficult. However, on the basis of the reactor runs and the evaluation, supposed critical parameters could be identified, which should be considered in a further approach.

5 Outlook

Further investigations of the individual interactions of the influencing factors during the refolding process could possibly lead to the development of a coherent model that includes the oxygen content, redox potential and reducing agent quantity. The resulting model has the potential to serve as a PAT tool. Based on these factors, it should also be possible to predict the free thiol concentration, which could be a CPP. If the free thiol concentration turns out to be a CPP, it could be used to improve the yield. A possible control could be via feeding cysteamine or a reducing agent such as TCEP. It would also be possible to feed the solubilisate into refolding buffer, as this initially results in lower protein concentrations, which often acts against aggregation. Furthermore, the redox potential can be kept low and cysteamine can be generated, since reducing agents can enter the reactor. In the field of refolding, mechanistic relationships have only been described to a limited extent and therefore linking CPPs with CQAs will be an important step in the future to improve low yields in the industry.

Bibliography

[1] Ahmad Alwosheel, Sander Van Cranenburgh, and Caspar G. Chorus. "Is your dataset big enough? Sample size requirements when using artificial neural networks for discrete choice analysis". en. In: *Journal of Choice Modelling* 28 (Sept. 2018), pp. 167–182. ISSN: 17555345. DOI: 10.1016/j.jocm.2018.07.002. URL: https://linkinghub.elsevier.com/retrieve/pii/S1755534518300058 (visited on 08/18/2023).

[2] Klaudia Arauzo-Aguilera et al. "Yields and product comparison between Escherichia coli BL21 and W3110 in industrially relevant conditions: anti-c-Met scFv as a case study". In: *Microbial Cell Factories* (May 2023). DOI: https://doi.org/10.1186/s12934âĂŚ023âĂŚ02111âĂŚ4.

[3] Jean-Philippe Arié et al. "Formation of active inclusion bodies in the periplasm of *Escherichia coli*: Active periplasmic inclusion bodies". en. In: *Molecular Microbiology* 62.2 (Oct. 2006), pp. 427–437. ISSN: 0950382X. DOI: 10.1111/j.1365-2958.2006.05394.x. URL: https://onlinelibrary.wiley.com/doi/10.1111/j.1365-2958.2006.05394.x (visited on 09/19/2023).

[4] Carla Atallah, Catherine Charcosset, and Hélène Greige-Gerges. "Challenges for cysteamine stabilization, quantification, and biological effects improvement". en. In: *Journal of Pharmaceutical Analysis* 10.6 (Dec. 2020), pp. 499–516. ISSN: 20951779. DOI: 10.1016/j.jpha.2020.03.007. URL: https://linkinghub.elsevier.com/retrieve/pii/S2095177919309025 (visited on 07/19/2023).

[5] Ruth E. Baker et al. "Mechanistic models versus machine learning, a fight worth fighting for the biological community?" en. In: *Biology Letters* 14.5 (May 2018), p. 20170660. ISSN: 1744-9561, 1744-957X. DOI: 10.1098/rsbl.2017.0660. URL: https://royalsocietypublishing.org/doi/10.1098/rsbl.2017.0660 (visited on 08/03/2023).

[6] Tyler J. Bechtel and Eranthie Weerapana. "From structure to redox: The diverse functional roles of disulfides and implications in disease". en. In: *PROTEOMICS* 17.6 (Mar. 2017), p. 1600391. ISSN: 16159853. DOI: 10.1002/pmic.201600391. URL: https://onlinelibrary.wiley.com/doi/10.1002/pmic.201600391 (visited on 06/17/2023).

[7] Ivano Bertini, ed. *Biological inorganic chemistry: structure and reactivity*. OCLC: ocm65400780. Sausalito, Calif: University Science Books, 2007. ISBN: 978-1-891389-43-6.

Bibliography

[8] Arshpreet Bhatwa et al. "Challenges Associated With the Formation of Recombinant Protein Inclusion Bodies in Escherichia coli and Strategies to Address Them for Industrial Applications". In: *Frontiers in Bioengineering and Biotechnology* 9 (Feb. 2021), p. 630551. ISSN: 2296-4185. DOI: 10.3389/fbioe.2021.630551. URL: https://www.frontiersin.org/articles/10.3389/fbioe.2021.630551/full (visited on 09/12/2023).

[9] *Biosimilars approved in Europe*. en. URL: https://www.gabionline.net/biosimilars/general/biosimilars-approved-in-europe (visited on 09/14/2023).

[10] *Biosimilars in der EU - Übersicht des vfa*. de. URL: https://www.vfa.de/de/arzneimittel-forschung/datenbanken-zu-arzneimitteln/biosimilars-uebersicht (visited on 09/14/2023).

[11] I. Bosnjak et al. "Occurrence of protein disulfide bonds in different domains of life: a comparison of proteins from the Protein Data Bank". en. In: *Protein Engineering Design and Selection* 27.3 (Mar. 2014), pp. 65–72. ISSN: 1741-0126, 1741-0134. DOI: 10.1093/protein/gzt063. URL: https://academic.oup.com/peds/article-lookup/doi/10.1093/protein/gzt063 (visited on 09/16/2023).

[12] Luisa Buscajoni et al. "Refolding in the modern biopharmaceutical industry". en. In: *Biotechnology Advances* 61 (Dec. 2022), p. 108050. ISSN: 07349750. DOI: 10.1016/j.biotechadv.2022.108050. URL: https://linkinghub.elsevier.com/retrieve/pii/S073497502200146X (visited on 06/17/2023).

[13] *C1QB - Complement C1q subcomponent subunit B - Homo sapiens (Human) | UniProtKB | UniProt*. URL: https://www.uniprot.org/uniprotkb/P02746/entry#ptm_processing (visited on 09/14/2023).

[14] Shmuel Cabilly. "Growth at sub-optimal temperatures allows the production of functional, antigen-binding Fab fragments in Escherichia coli". en. In: *Gene* 85.2 (Dec. 1989), pp. 553–557. ISSN: 03781119. DOI: 10.1016/0378-1119(89)90451-4. URL: https://linkinghub.elsevier.com/retrieve/pii/0378111989904514 (visited on 09/12/2023).

[15] Lisa D. Cabrita and Stephen P. Bottomley. "Protein expression and refolding – A practical guide to getting the most out of inclusion bodies". en. In: *Biotechnology Annual Review*. Vol. 10. Elsevier, 2004, pp. 31–50. ISBN: 978-0-444-51749-4. DOI: 10.1016/S1387-2656(04)10002-1. URL: https://linkinghub.elsevier.com/retrieve/pii/S1387265604100021 (visited on 06/17/2023).

[16] M.Mar Carrió, Rafael Cubarsi, and Antonio Villaverde. "Fine architecture of bacterial inclusion bodies". en. In: *FEBS Letters* 471.1 (Apr. 2000), pp. 7–11. ISSN: 0014-5793, 1873-3468. DOI: 10.1016/S0014-5793(00)01357-0. URL: https://febs.onlinelibrary.wiley.com/doi/10.1016/S0014-5793%2800%2901357-0 (visited on 09/19/2023).

[17] Kc Chaluvaraju et al. "Review of insulin and its analogues in diabetes mellitus". en. In: *Journal of Basic and Clinical Pharmacy* 3.2 (2012), p. 283. ISSN: 0976-0105. DOI: 10.4103/0976-0105.103822. URL: http://www.jbclinpharm.org/text.asp?2012/3/2/283/103822 (visited on 09/14/2023).

[18] M. O. Chaney and L. K. Steinrauf. “The crystal and molecular structure of tetragonal L -cystine”. In: *Acta Crystallographica Section B Structural Crystallography and Crystal Chemistry* 30.3 (Mar. 1974), pp. 711–716. ISSN: 0567-7408. DOI: 10.1107/S0567740874003566. URL: https://scripts.iucr.org/cgi-bin/paper?S0567740874003566 (visited on 09/16/2023).

[19] Chunfang Chang et al. “Optimization of tris(2-carboxyethyl) phosphine reduction conditions for fast analysis of total biothiols in mouse serum samples”. en. In: *Heliyon* 5.5 (May 2019), e01598. ISSN: 24058440. DOI: 10.1016/j.heliyon.2019.e01598. URL: https://linkinghub.elsevier.com/retrieve/pii/S2405844018391722 (visited on 07/20/2023).

[20] R E Childs and W G Bardsley. “The steady-state kinetics of peroxidase with 2,2-azino-di-(3-ethyl-benzthiazoline-6-sulphonic acid) as chromogen”. en. In: *Biochemical Journal* 145.1 (Jan. 1975), pp. 93–103. ISSN: 0264-6021. DOI: 10.1042/bj1450093. URL: https://portlandpress.com/biochemj/article/145/1/93/8988/The-steady-state-kinetics-of-peroxidase-with-2-2 (visited on 07/04/2023).

[21] J.R Clarkson, Z.F Cui, and R.C Darton. “Protein Denaturation in Foam”. en. In: *Journal of Colloid and Interface Science* 215.2 (July 1999), pp. 323–332. ISSN: 00219797. DOI: 10.1006/jcis.1999.6255. URL: https://linkinghub.elsevier.com/retrieve/pii/S0021979799962550 (visited on 06/23/2023).

[22] Ian Clegg. “Process analytical technology”. en. In: *Specification of Drug Substances and Products*. Elsevier, 2020, pp. 149–173. ISBN: 978-0-08-102824-7. DOI: 10.1016/B978-0-08-102824-7.00007-5. URL: https://linkinghub.elsevier.com/retrieve/pii/B9780081028247000075 (visited on 09/18/2023).

[23] J.L. Cleland, C Hedgepeth, and D.I. Wang. “Polyethylene glycol enhanced refolding of bovine carbonic anhydrase B. Reaction stoichiometry and refolding model.” en. In: *Journal of Biological Chemistry* 267.19 (July 1992), pp. 13327–13334. ISSN: 00219258. DOI: 10.1016/S0021-9258(18)42214-4. URL: https://linkinghub.elsevier.com/retrieve/pii/S0021925818422144 (visited on 07/27/2023).

[24] *CONMIN — pyOptSparse documentation*. URL: https://mdolab-pyoptsparse.readthedocs-hosted.com/en/latest/optimizers/CONMIN.html (visited on 08/05/2023).

[25] Jipeng Di, Bingbing Liu, and Xianliang Song. “The Galactose Oxidase Air Oxidation of Galactomannans for Use as Paper Strengthening Agents”. en. In: *Journal of Wood Chemistry and Technology* 40.2 (Mar. 2020), pp. 105–115. ISSN: 0277-3813, 1532-2319. DOI: 10.1080/02773813.2019.1661486. URL: https://www.tandfonline.com/doi/full/10.1080/02773813.2019.1661486 (visited on 06/27/2023).

[26] Ken A. Dill and Hue Sun Chan. "From Levinthal to pathways to funnels". en. In: *Nature Structural & Molecular Biology* 4.1 (Jan. 1997), pp. 10–19. ISSN: 1545-9993, 1545-9985. DOI: 10.1038/nsb0197-10. URL: https://www.nature.com/doifinder/10.1038/nsb0197-10 (visited on 07/27/2023).

[27] Yadolah Dodge. *The concise encyclopedia of statistics*. 1st. ed. Springer reference. New York: Springer, 2008. ISBN: 978-0-387-31742-7 978-0-387-32833-1 978-0-387-33828-6.

[28] Steven D. Doig et al. "Modelling surface aeration rates in shaken microtitre plates using dimensionless groups". en. In: *Chemical Engineering Science* 60.10 (May 2005), pp. 2741–2750. ISSN: 00092509. DOI: 10.1016/j.ces.2004.12.025. URL: https://linkinghub.elsevier.com/retrieve/pii/S0009250905000102 (visited on 09/21/2023).

[29] X.-Y. Dong et al. "Modeling and Simulation of Fed-Batch Protein Refolding Proces". en. In: *Biotechnology Progress* 20.4 (Aug. 2004), pp. 1213–1219. ISSN: 8756-7938. DOI: 10.1021/bp0499597. URL: http://doi.wiley.com/10.1021/bp0499597 (visited on 07/27/2023).

[30] *ELANE - Neutrophil elastase - Homo sapiens (Human) | UniProtKB | UniProt*. URL: https://www.uniprot.org/uniprotkb/P08246/entry#ptm_processing (visited on 09/14/2023).

[31] Beatrix Fahnert, Hauke Lilie, and Peter Neubauer. "Inclusion Bodies: Formation and Utilisation". In: *Physiological Stress Responses in Bioprocesses*. Vol. 89. Series Title: Advances in Biochemical Engineering/Biotechnology. Berlin, Heidelberg: Springer Berlin Heidelberg, Apr. 2004, pp. 93–142. ISBN: 978-3-540-20311-7 978-3-540-39669-7. DOI: 10.1007/b93995. URL: http://link.springer.com/10.1007/b93995 (visited on 06/13/2023).

[32] Bernhard Fischer, Ian Sumner, and Peter Goodenough. "Isolation, renaturation, and formation of disulfide bonds of eukaryotic proteins expressed inEscherichia coli as inclusion bodies". en. In: *Biotechnology and Bioengineering* 41.1 (Jan. 1993), pp. 3–13. ISSN: 0006-3592, 1097-0290. DOI: 10.1002/bit.260410103. URL: https://onlinelibrary.wiley.com/doi/10.1002/bit.260410103 (visited on 09/16/2023).

[33] Bernhard Fischer et al. "A novel sequential procedure to enhance the renaturation of recombinant protein from *Escherichia coil* inclusion bodies". en. In: *"Protein Engineering, Design and Selection"* 5.6 (1992), pp. 593–596. ISSN: 1741-0126, 1741-0134. DOI: 10.1093/protein/5.6.593. URL: https://academic.oup.com/peds/article-lookup/doi/10.1093/protein/5.6.593 (visited on 09/19/2023).

[34] *GAOA - Galactose oxidase - Gibberella zeae (Wheat head blight fungus) | UniProtKB | UniProt*. URL: https://www.uniprot.org/uniprotkb/P0CS93/entry (visited on 03/09/2023).

[35] Felix Garcia-Ochoa and Emilio Gomez. "Oxygen Transfer Rate Determination: Chemical, Physical and Biological Methods". en. In: *Encyclopedia of Industrial Biotechnology*. 1st ed. Wiley, Apr. 2010, pp. 1–21. ISBN: 978-0-471-79930-6 978-0-470-05458-1. DOI: 10.1002/9780470054581.eib467. URL: https://onlinelibrary.wiley.com/doi/10.1002/9780470054581.eib467 (visited on 09/26/2023).

[36] "Guidance for Industry PAT - A Framework for Innovative Pharmaceutical Development, manufacturing, and Quality Assurance". en. In: ().

[37] Thomas Gundinger and Oliver Spadiut. "A comparative approach to recombinantly produce the plant enzyme horseradish peroxidase in Escherichia coli". en. In: *Journal of Biotechnology* 248 (Apr. 2017), pp. 15–24. ISSN: 01681656. DOI: 10.1016/j.jbiotec.2017.03.003. URL: https://linkinghub.elsevier.com/retrieve/pii/S0168165617301013 (visited on 09/12/2023).

[38] J.C. Han and G.Y. Han. "A Procedure for Quantitative Determination of Tris(2-Carboxyethyl)phosphine, an Odorless Reducing Agent More Stable and Effective Than Dithiothreitol". en. In: *Analytical Biochemistry* 220.1 (July 1994), pp. 5–10. ISSN: 00032697. DOI: 10.1006/abio.1994.1290. URL: https://linkinghub.elsevier.com/retrieve/pii/S0003269784712905 (visited on 03/03/2023).

[39] Diane L. Hevehan and Eliana De Bernardez Clark. "Oxidative renaturation of lysozyme at high concentrations". en. In: *Biotechnology and Bioengineering* 54.3 (May 1997), pp. 221–230. ISSN: 00063592, 10970290. DOI: 10.1002/(SICI)1097-0290(19970505)54:3<221::AID-BIT3>3.0.CO;2-H. URL: https://onlinelibrary.wiley.com/doi/10.1002/(SICI)1097-0290(19970505)54:3%3C221::AID-BIT3%3E3.0.CO;2-H (visited on 07/27/2023).

[40] Fahmi Himo et al. "Catalytic Mechanism of Galactose Oxidase: A Theoretical Study". en. In: *Journal of the American Chemical Society* 122.33 (Aug. 2000), pp. 8031–8036. ISSN: 0002-7863, 1520-5126. DOI: 10.1021/ja994527r. URL: https://pubs.acs.org/doi/10.1021/ja994527r (visited on 06/27/2023).

[41] F. Hoffmann and U. Rinas. "Kinetics of Heat-Shock Response and Inclusion Body Formation During Temperature-Induced Production of Basic Fibroblast Growth Factor in High-Cell-Density Cultures of Recombinant Escherichia coli". en. In: *Biotechnology Progress* 16.6 (Dec. 2000), pp. 1000–1007. ISSN: 8756-7938. DOI: 10.1021/bp0000959. URL: http://doi.wiley.com/10.1021/bp0000959 (visited on 09/12/2023).

[42] Devin A. Hudson, Shawn A. Gannon, and Colin Thorpe. "Oxidative protein folding: From thiol–disulfide exchange reactions to the redox poise of the endoplasmic reticulum". en. In: *Free Radical Biology and Medicine* 80 (Mar. 2015), pp. 171–182. ISSN: 08915849. DOI: 10.1016/j.freeradbiomed.2014.07.037. URL: https://linkinghub.elsevier.com/retrieve/pii/S0891584914003542 (visited on 06/23/2023).

Bibliography

[43] Baolei Jia and Che Ok Jeon. "High-throughput recombinant protein expression in *Escherichia coli* : current status and future perspectives". en. In: *Open Biology* 6.8 (Aug. 2016), p. 160196. ISSN: 2046-2441. DOI: 10.1098/rsob.160196. URL: https://royalsocietypublishing.org/doi/10.1098/rsob.160196 (visited on 05/24/2023).

[44] Alois Jungbauer and Waltraud Kaar. "Current status of technical protein refolding". en. In: *Journal of Biotechnology* 128.3 (Feb. 2007), pp. 587–596. ISSN: 01681656. DOI: 10.1016/j.jbiotec.2006.12.004. URL: https://linkinghub.elsevier.com/retrieve/pii/S0168165606010273 (visited on 07/27/2023).

[45] Britta Jürgen et al. "Quality control of inclusion bodies in Escherichia coli". en. In: *Microbial Cell Factories* 9.1 (Dec. 2010), p. 41. ISSN: 1475-2859. DOI: 10.1186/1475-2859-9-41. URL: https://microbialcellfactories.biomedcentral.com/articles/10.1186/1475-2859-9-41 (visited on 09/12/2023).

[46] T. Kenzom, P. Srivastava, and S. Mishra. "Structural Insights into 2,2-Azino-Bis(3-Ethylbenzothiazoline-6-Sulfonic Acid) (ABTS)-Mediated Degradation of Reactive Blue 21 by Engineered Cyathus bulleri Laccase and Characterization of Degradation Products". en. In: *Applied and Environmental Microbiology* 80.24 (Dec. 2014). Ed. by D. Cullen, pp. 7484–7495. ISSN: 0099-2240, 1098-5336. DOI: 10.1128/AEM.02665-14. URL: https://journals.asm.org/doi/10.1128/AEM.02665-14 (visited on 07/17/2023).

[47] Thomas Kiefhaber et al. "Protein Aggregation in vitro and in vivo: A Quantitative Model of the Kinetic Competition between Folding and Aggregation". en. In: *Nature Biotechnology* 9.9 (Sept. 1991), pp. 825–829. ISSN: 1087-0156, 1546-1696. DOI: 10.1038/nbt0991-825. URL: https://www.nature.com/doifinder/10.1038/nbt0991-825 (visited on 07/27/2023).

[48] Julian Kopp et al. "Development of a generic reversed-phase liquid chromatography method for protein quantification using analytical quality-by-design principles". en. In: *Journal of Pharmaceutical and Biomedical Analysis* 188 (Sept. 2020), p. 113412. ISSN: 07317085. DOI: 10.1016/j.jpba.2020.113412. URL: https://linkinghub.elsevier.com/retrieve/pii/S073170852031298X (visited on 09/05/2023).

[49] Th. Kopp. "Blasenfreie Begasung". de. In: *Acta Biotechnologica* 9.6 (1989), pp. 504–511. ISSN: 0138-4988, 1521-3846. DOI: 10.1002/abio.370090603. URL: https://onlinelibrary.wiley.com/doi/10.1002/abio.370090603 (visited on 09/21/2023).

[50] Jashwant Kumar, Sami U. Bhat, and Anurag S. Rathore. "Slow post-induction specific growth rate enhances recombinant protein expression in Escherichia coli: Pramlintide multimer and ranibizumab production as case studies". en. In: *Process Biochemistry* 114 (Mar. 2022), pp. 21–27. ISSN: 13595113. DOI: 10.1016/j.procbio.2022.01.009. URL: https://linkinghub.elsevier.com/retrieve/pii/S1359511322000150 (visited on 09/12/2023).

[51] Wenjin Li, Ilona B. Baldus, and Frauke Gräter. "Redox Potentials of Protein Disulfide Bonds from Free-Energy Calculations". en. In: *The Journal of Physical Chemistry B* 119.17 (Apr. 2015), pp. 5386–5391. ISSN: 1520-6106, 1520-5207. DOI: 10.1021/acs.jpcb.5b01051. URL: https://pubs.acs.org/doi/10.1021/acs.jpcb.5b01051 (visited on 06/22/2023).

[52] Octavio Loyola-Gonzalez. "Black-Box vs. White-Box: Understanding Their Advantages and Weaknesses From a Practical Point of View". In: *IEEE Access* 7 (2019), pp. 154096–154113. ISSN: 2169-3536. DOI: 10.1109/ACCESS.2019.2949286. URL: https://ieeexplore.ieee.org/document/8882211/ (visited on 08/03/2023).

[53] Angélica Meneses-Acosta et al. "Effect of controlled redox potential and dissolved oxygen on the in vitro refolding of an E. coli alkaline phosphatase and chicken lysozyme". en. In: *Enzyme and Microbial Technology* 52.6-7 (May 2013), pp. 312–318. ISSN: 01410229. DOI: 10.1016/j.enzmictec.2013.03.008. URL: https://linkinghub.elsevier.com/retrieve/pii/S0141022913000483 (visited on 06/13/2023).

[54] Hugo G Menzella, Hugo C Gramajo, and Eduardo A Ceccarelli. "High recovery of prochymosin from inclusion bodies using controlled air oxidation". en. In: *Protein Expression and Purification* 25.2 (July 2002), pp. 248–255. ISSN: 10465928. DOI: 10.1016/S1046-5928(02)00006-2. URL: https://linkinghub.elsevier.com/retrieve/pii/S1046592802000062 (visited on 09/05/2023).

[55] Seyed Babak Mousavi et al. "Development of a two-step refolding method for reteplase, a rich disulfide-bonded protein". en. In: *Process Biochemistry* 74 (Nov. 2018), pp. 94–102. ISSN: 13595113. DOI: 10.1016/j.procbio.2018.05.006. URL: https://linkinghub.elsevier.com/retrieve/pii/S1359511318301703 (visited on 09/16/2023).

[56] Paola Nieri et al. "Cholinesterase-like organocatalysis by imidazole and imidazole-bearing molecules". en. In: *Scientific Reports* 7.1 (Apr. 2017), p. 45760. ISSN: 2045-2322. DOI: 10.1038/srep45760. URL: https://www.nature.com/articles/srep45760 (visited on 07/19/2023).

[57] Siqi Pan et al. "Engineering batch and pulse refolding with transition of aggregation kinetics: An investigation using green fluorescent protein (GFP)". en. In: *Chemical Engineering Science* 131 (July 2015), pp. 91–100. ISSN: 00092509. DOI: 10.1016/j.ces.2015.03.054. URL: https://linkinghub.elsevier.com/retrieve/pii/S0009250915002353 (visited on 07/27/2023).

[58] Jan Niklas Pauk et al. "Advances in monitoring and control of refolding kinetics combining PAT and modeling". en. In: *Applied Microbiology and Biotechnology* 105.6 (Mar. 2021), pp. 2243–2260. ISSN: 0175-7598, 1432-0614. DOI: 10.1007/s00253-021-11151-y. URL: http://link.springer.com/10.1007/s00253-021-11151-y (visited on 07/27/2023).

[59] *PTH1R - Parathyroid hormone/parathyroid hormone-related peptide receptor - Homo sapiens (Human) | UniProtKB | UniProt*. URL: https://www.uniprot.org/uniprotkb/Q03431/entry#ptm_processing (visited on 09/14/2023).

[60] Hanshi N. Qi et al. "Experimental and Theoretical Analysis of Tubular Membrane Aeration for Mammalian Cell Bioreactors". en. In: *Biotechnology Progress* 19.4 (Sept. 2008), pp. 1183–1189. ISSN: 87567938. DOI: 10.1021/bp025780p. URL: http://doi.wiley.com/10.1021/bp025780p (visited on 09/21/2023).

[61] Ana Ramón, Mario Señorale-Pose, and Mónica Marín. "Inclusion bodies: not that bad..." In: *Frontiers in Microbiology* 5 (2014). ISSN: 1664-302X. DOI: 10.3389/fmicb.2014.00056. URL: http://journal.frontiersin.org/article/10.3389/fmicb.2014.00056/abstract (visited on 05/24/2023).

[62] *Recombinant Proteins Market Size & Growth Report, 2030*. en. URL: https://www.grandviewresearch.com/industry-analysis/recombinant-proteins-market-report (visited on 09/05/2023).

[63] Melanie S. Rogers et al. "Cross-Link Formation of the Cysteine 228Tyrosine 272 Catalytic Cofactor of Galactose Oxidase Does Not Require Dioxygen". en. In: *Biochemistry* 47.39 (Sept. 2008), pp. 10428–10439. ISSN: 0006-2960, 1520-4995. DOI: 10.1021/bi8010835. URL: https://pubs.acs.org/doi/10.1021/bi8010835 (visited on 07/06/2023).

[64] GermÃ¡n L. Rosano and Eduardo A. Ceccarelli. "Recombinant protein expression in Escherichia coli: advances and challenges". In: *Frontiers in Microbiology* 5 (Apr. 2014). ISSN: 1664-302X. DOI: 10.3389/fmicb.2014.00172. URL: http://journal.frontiersin.org/article/10.3389/fmicb.2014.00172/abstract (visited on 05/24/2023).

[65] Henry Roth, Stanton Segal, and Dolores Bertoli. "The quantitative determination of galactose—An enzymic method using galactose oxidase, with applications to blood and other biological fluids". en. In: *Analytical Biochemistry* 10.1 (Jan. 1965), pp. 32–52. ISSN: 00032697. DOI: 10.1016/0003-2697(65)90238-1. URL: https://linkinghub.elsevier.com/retrieve/pii/0003269765902381 (visited on 06/27/2023).

[66] Sylwia Ryś et al. "Design and optimization of protein refolding with crossflow ultrafiltration". en. In: *Chemical Engineering Science* 130 (July 2015), pp. 290–300. ISSN: 00092509. DOI: 10.1016/j.ces.2015.03.035. URL: https://linkinghub.elsevier.com/retrieve/pii/S0009250915002079 (visited on 07/27/2023).

[67] Walkiria S. Schlindwein and Mark Gibson, eds. *Pharmaceutical quality by design: a practical approach*. First edition. Advances in pharmaceutical technology. Hoboken, NJ: John Wiley & Sons, 2018. ISBN: 978-1-118-89522-1 978-1-118-89521-4.

[68] M. Schneider et al. "Bubble-free oxygenation by means of hydrophobic porous membranes". en. In: *Enzyme and Microbial Technology* 17.9 (Sept. 1995), pp. 839–847. ISSN: 01410229. DOI: 10.1016/0141-0229(94)00113-6. URL: https://linkinghub.elsevier.com/retrieve/pii/0141022994001136 (visited on 09/21/2023).

[69] AbulKalam M Shamsuddin. "A Simple Screening Test for Cancer". In: *Advances in Cancer Research & Clinical Imaging* 3.2 (Apr. 2021). ISSN: 26888203. DOI: 10.33552/ACRCI.2021.03.000558. URL: https://irispublishers.com/acrci/fulltext/a-simple-screening-test-for-cancer.ID.000558.php (visited on 06/27/2023).

[70] Yumiko Shirano and Daisuke Shibata. "Low temperature cultivation of *Escherichia coli* carrying a rice lipoxygenase L-2 cDNA produces a soluble and active enzyme at a high level". en. In: *FEBS Letters* 271.1-2 (Oct. 1990), pp. 128–130. ISSN: 00145793. DOI: 10.1016/0014-5793(90)80388-Y. URL: http://doi.wiley.com/10.1016/0014-5793%2890%2980388-Y (visited on 09/12/2023).

[71] Anupam Singh et al. "Protein recovery from inclusion bodies of Escherichia coli using mild solubilization process". en. In: *Microbial Cell Factories* 14.1 (Dec. 2015), p. 41. ISSN: 1475-2859. DOI: 10.1186/s12934-015-0222-8. URL: https://microbialcellfactories.biomedcentral.com/articles/10.1186/s12934-015-0222-8 (visited on 06/13/2023).

[72] Anupam Singh et al. "Structure-Function Relationship of Inclusion Bodies of a Multimeric Protein". In: *Frontiers in Microbiology* 11 (May 2020), p. 876. ISSN: 1664-302X. DOI: 10.3389/fmicb.2020.00876. URL: https://www.frontiersin.org/article/10.3389/fmicb.2020.00876/full (visited on 06/13/2023).

[73] Christoph Slouka et al. "Perspectives of inclusion bodies for bio-based products: curse or blessing?" en. In: *Applied Microbiology and Biotechnology* 103.3 (Feb. 2019), pp. 1143–1153. ISSN: 0175-7598, 1432-0614. DOI: 10.1007/s00253-018-9569-1. URL: http://link.springer.com/10.1007/s00253-018-9569-1 (visited on 05/24/2023).

[74] Tuomas E. Tahko. "The modal basis of scientific modelling". en. In: *Synthese* 201.3 (Feb. 2023), p. 75. ISSN: 1573-0964. DOI: 10.1007/s11229-023-04063-z. URL: https://link.springer.com/10.1007/s11229-023-04063-z (visited on 07/27/2023).

[75] "International Conference On Harmonisation Of Technical Requirements For Registration Of Pharmaceuticals For Human Use". en. In: *Handbook of Transnational Economic Governance Regimes*. Ed. by Christian Tietje and Alan Brouder. Brill | Nijhoff, Jan. 2010, pp. 1041–1053. ISBN: 978-90-04-18156-4 978-90-04-16330-0. DOI: 10.1163/ej.9789004163300.i-1081.897. URL: https://brill.com/view/book/edcoll/9789004181564/Bej.9789004163300.i-1081_085.xml (visited on 09/18/2023).

[76] *TNF - Tumor necrosis factor - Homo sapiens (Human) | UniProtKB | UniProt*. URL: https://www.uniprot.org/uniprotkb/P01375/entry#ptm_processing (visited on 09/14/2023).

[77] Paul S. Tressel and Daniel J. Kosman. "[27] Galactose oxidase from Dactylium dendroides". en. In: *Methods in Enzymology*. Vol. 89. Elsevier, 1982, pp. 163–171. ISBN: 978-0-12-181989-7. DOI: 10.1016/S0076-6879(82)89029-0. URL: https://linkinghub.elsevier.com/retrieve/pii/S0076687982890290 (visited on 07/04/2023).

[78] Nagesh K. Tripathi and Ambuj Shrivastava. "Recent Developments in Bioprocessing of Recombinant Proteins: Expression Hosts and Process Development". In: *Frontiers in Bioengineering and Biotechnology* 7 (Dec. 2019), p. 420. ISSN: 2296-4185. DOI: 10.3389/fbioe.2019.00420. URL: https://www.frontiersin.org/article/10.3389/fbioe.2019.00420/full (visited on 09/12/2023).

[79] Kouhei Tsumoto et al. "Practical considerations in refolding proteins from inclusion bodies". en. In: *Protein Expression and Purification* 28.1 (Mar. 2003), pp. 1–8. ISSN: 10465928. DOI: 10.1016/S1046-5928(02)00641-1. URL: https://linkinghub.elsevier.com/retrieve/pii/S1046592802006411 (visited on 09/19/2023).

[80] Nj. Turner. "7.12 Oxidation: Oxidases". en. In: *Comprehensive Chirality*. Elsevier, 2012, pp. 256–274. ISBN: 978-0-08-095168-3. DOI: 10.1016/B978-0-08-095167-6.00715-1. URL: https://linkinghub.elsevier.com/retrieve/pii/B9780080951676007151 (visited on 06/27/2023).

[81] Salman Sadullah Usmani et al. "THPdb: Database of FDA-approved peptide and protein therapeutics". en. In: *PLOS ONE* 12.7 (July 2017). Ed. by Qing-Xiang Amy Sang, e0181748. ISSN: 1932-6203. DOI: 10.1371/journal.pone.0181748. URL: https://dx.plos.org/10.1371/journal.pone.0181748 (visited on 09/05/2023).

[82] *VEGFA - Vascular endothelial growth factor A, long form - Homo sapiens (Human) | UniProtKB | UniProt*. URL: https://www.uniprot.org/uniprotkb/P15692/entry#ptm_processing (visited on 09/14/2023).

[83] P. Walstra. "Principles of Foam Formation and Stability". In: *Foams: Physics, Chemistry and Structure*. Ed. by Anthony William Robards and Ashley Wilson. Series Title: Springer Series in Applied Biology. London: Springer London, 1989, pp. 1–15. ISBN: 978-1-4471-3809-9 978-1-4471-3807-5. DOI: 10.1007/978-1-4471-3807-5_1. URL: http://link.springer.com/10.1007/978-1-4471-3807-5_1 (visited on 09/19/2023).

[84] James W. Whittaker. "The radical chemistry of galactose oxidase". en. In: *Archives of Biochemistry and Biophysics* 433.1 (Jan. 2005), pp. 227–239. ISSN: 00039861. DOI: 10.1016/j.abb.2004.08.034. URL: https://linkinghub.elsevier.com/retrieve/pii/S0003986104005156 (visited on 06/27/2023).

[85] Christoph Wiedemann et al. "Cysteines and Disulfide Bonds as Structure-Forming Units: Insights From Different Domains of Life and the Potential for Characterization by NMR". In: *Frontiers in Chemistry* 8 (Apr. 2020), p. 280. ISSN: 2296-2646. DOI: 10.3389/fchem.2020.00280. URL: https://www.frontiersin.org/article/10.3389/fchem.2020.00280/full (visited on 09/16/2023).

[86] Svante Wold, Michael Sjöström, and Lennart Eriksson. "PLS-regression: a basic tool of chemometrics". en. In: *Chemometrics and Intelligent Laboratory Systems* 58.2 (Oct. 2001), pp. 109–130. ISSN: 01697439. DOI: 10.1016/S0169-7439(01)00155-1. URL: https://linkinghub.elsevier.com/retrieve/pii/S0169743901001551 (visited on 08/18/2023).

[87] Yiming Xiao and Lars Konermann. "Protein structural dynamics at the gas/water interface examined by hydrogen exchange mass spectrometry: Protein Dynamics at Gas/Water Interfaces". en. In: *Protein Science* 24.8 (Aug. 2015), pp. 1247–1256. ISSN: 09618368. DOI: 10.1002/pro.2680. URL: https://onlinelibrary.wiley.com/doi/10.1002/pro.2680 (visited on 03/08/2023).

[88] F.-C. Yang and C.-B. Liau. "Effects of cultivating conditions on the mycelial growth of Ganoderma lucidum in submerged flask cultures". en. In: *Bioprocess Engineering* 19.3 (Sept. 1998), pp. 233–236. ISSN: 0178-515X. DOI: 10.1007/PL00009014. URL: http://link.springer.com/10.1007/PL00009014 (visited on 09/21/2023).

[89] Xueqing Yang and Yalin Zhang. "Effect of temperature and sorbitol in improving the solubility of carboxylesterases protein CpCE-1 from Cydia pomonella and biochemical characterization". en. In: *Applied Microbiology and Biotechnology* 97.24 (Dec. 2013), pp. 10423–10433. ISSN: 0175-7598, 1432-0614. DOI: 10.1007/s00253-013-5236-8. URL: http://link.springer.com/10.1007/s00253-013-5236-8 (visited on 09/12/2023).

[90] Gerd Zettlmeissl, Rainer Rudolph, and Rainer Jaenicke. "Reconstitution of lactic dehydrogenase. Noncovalent aggregation vs. reactivation. 1. Physical properties and kinetics of aggregation". en. In: *Biochemistry* 18.25 (Dec. 1979), pp. 5567–5571. ISSN: 0006-2960, 1520-4995. DOI: 10.1021/bi00592a007. URL: https://pubs.acs.org/doi/abs/10.1021/bi00592a007 (visited on 07/27/2023).

[91] Ting Zhang et al. "Modeling of protein refolding from inclusion bodies". en. In: *Acta Biochimica et Biophysica Sinica* 41.12 (Dec. 2009), pp. 1044–1052. ISSN: 1672-9145. DOI: 10.1093/abbs/gmp098. URL: http://engine.scichina.com/doi/10.1093/abbs/gmp098 (visited on 09/12/2023).

[92] Wangang Zhang, Shan Xiao, and Dong U. Ahn. "Protein Oxidation: Basic Principles and Implications for Meat Quality". en. In: *Critical Reviews in Food Science and Nutrition* 53.11 (Jan. 2013), pp. 1191–1201. ISSN: 1040-8398, 1549-7852. DOI: 10.1080/10408398.2011.577540. URL: http://www.tandfonline.com/doi/abs/10.1080/10408398.2011.577540 (visited on 10/04/2023).

List of Figures

List of Figures

List of Tables

Appendix

Table 5.1: Biosimilars approved by the EU in 2021-2022[10, 9]

Product name	Active substance	Authorization date	Manufacturer /Company name	Disulfid bond
Abevmy	bevacizumab	21. Apr 2021	Mylan (now Viatris)	Yes[13]
Alymsys	bevacizumab	26. Mar 2021	mAbxience Research	Yes[13]
Byooviz	ranibizumab	18. Aug 2021	Samsung Bioepis	Yes[82]
Hukyndra	adalimumab	15. Nov 2021	Alvotech /Stada Artnimettel	Yes[76]
Kirsty	insulin aspart	05. Feb 2021	Biocon /Viatris	Yes[17]
Libmyris	adalimumab	12. Nov 2021	Alvotech /Stada Artnimettel	Yes[76]
Onbevzi	bevacizumab	11. Jan 2021	Samsung Bioepis	Yes[13]
Oyavas	bevacizumab	26 Mar 2021	Stada Arzneimittel	Yes[13]
Yuflyma	adalimumab	11. Feb 2021	Celltrion Healthcare	Yes[76]
Ranivisio	ranibizumab	25. Aug 2022	Bioeq/Teva Pharma	Yes[82]
Sondelbay	teriparatide	24. Mar 2022	Accord Healthcare	Yes[59]
Stimufend	pegfilgrastim	24. Mar 2022	Fresenius Kabi	Yes[30]
Truvelog Mix 30	insulin aspart	Apr 2022	Sanofi-Aventis	Yes[17]
Vegzelma	bevacizumab	17. Aug 2022	Celltrion Healthcare	Yes[13]
Ximluci	ranibizumab	09. Nov 2022	Stada Arzneimittel /Xbrane Biopharma	Yes[82]

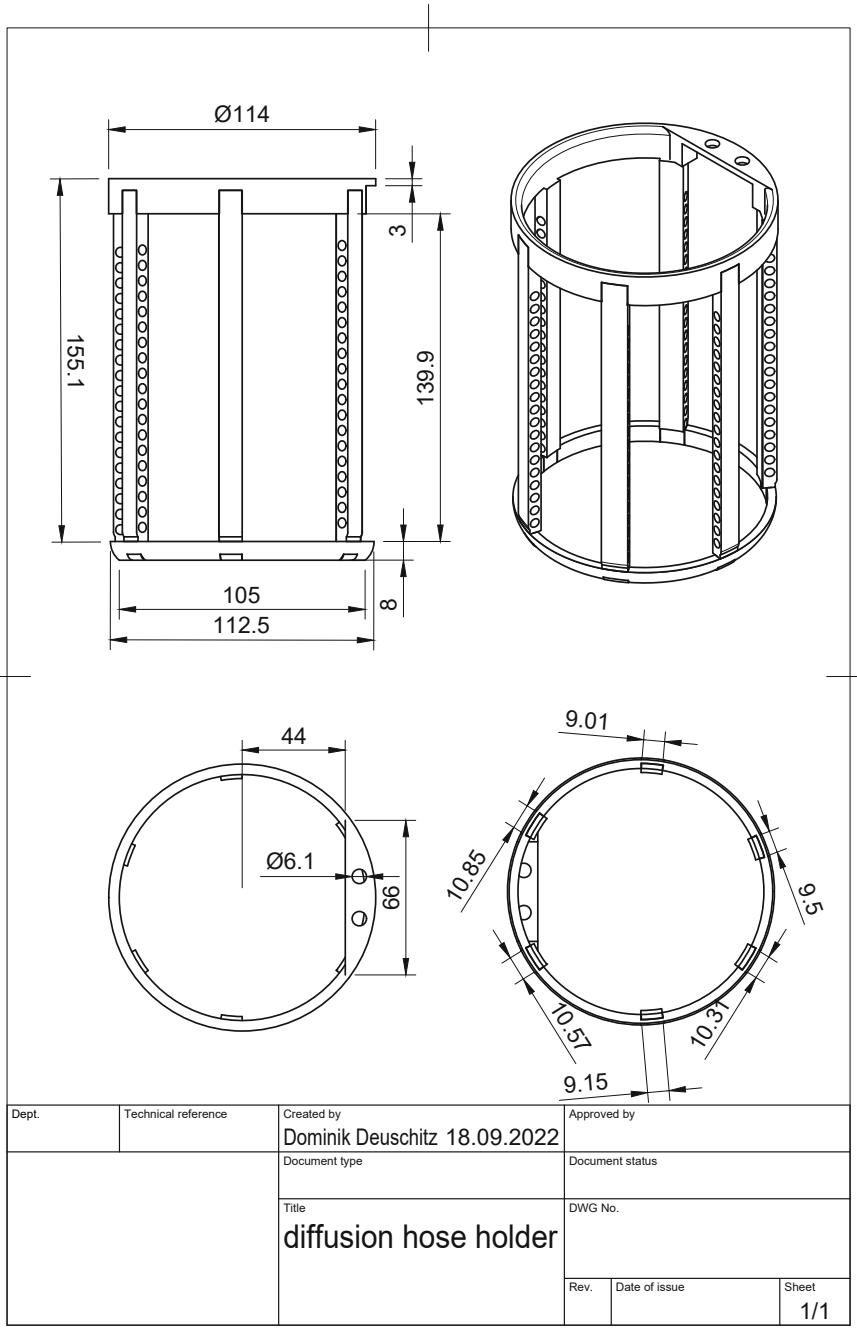

Figure 5.1: Detailed sketch of diffusion hose holder

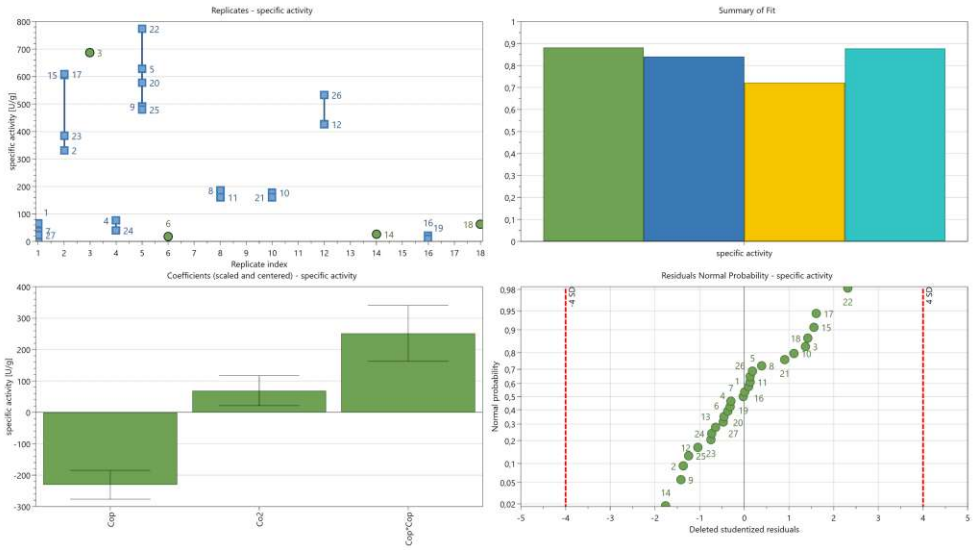

Figure 5.2: Representation of the summara plot of MODDE for the created DoE model.

Table 5.2: Data of the statistical evaluation of the protein concentration of all reactor runs divided into two groups. Data from 0-12 h and from 20-27 h.

run name	mean 0-12 h [g L^{-1}]	mean 20-27 h [g L^{-1}]	std 0-12 h [g L^{-1}]	std 20-27 h [g L^{-1}]	Levene-test [p-value]	Test on equivalent means [p-value]
DO0 & Redox-300	0.75	0.77	0.017	0.038	0.17	0.29
DO30	0.60	0.63	0.053	0.039	0.45	0.13
DO80	0.74	0.75	0.011	0.017	0.03	0.78
DO120	0.73	0.74	0.014	0.024	0.09	0.07
Redox-200	0.42	0.43	0.072	0.049	0.40	0.90
Redox-150	0.69	0.69	0.047	0.026	0.23	0.85